European Journal of Medicinal Chemistry 191 (2020) 112140

Contents lists available at ScienceDirect

European Journal of Medicinal Chemistry

journal homepage: http://www.elsevier.com/locate/ejmech

Research paper

Design, synthesis and biological evaluation of 2,3-dihydro-5,6-dimethoxy-1*H*-inden-1-one and piperazinium salt hybrid derivatives as hAChE and hBuChE enzyme inhibitors

Sakineh Mozaffarnia [a, b], Reza Teimuri-Mofrad [a, *], Mohammad-Reza Rashidi [b]

[a] Department of Organic and Biochemistry, Faculty of Chemistry, University of Tabriz, Tabriz, Iran
[b] Research Center for Pharmaceutical Nanotechnology, Tabriz University of Medical Sciences, Tabriz, Iran

ARTICLE INFO

Article history:
Received 31 December 2019
Received in revised form
9 February 2020
Accepted 9 February 2020
Available online 13 February 2020

Keywords:
Alzheimer's disease
Dual inhibition
AChE
BuChE
Molecular modeling

ABSTRACT

2,3-Dihydro-5,6-dimethoxy-2-[4-(4-alkyl-4-methylpiperazinium-1-yl)benzylidine]-1*H*-inden-1-one halide salt derivatives as a novel donepezil hybrid analogs with the property of acetylcholinesterase (AChE) and butyrylcholinesterase (BuChE) enzyme inhibition were designed and synthesized via N-alkylation reaction of 2,3-dihydro-5,6-dimethoxy-2-[4-(4-methylpiperazin-1-yl)benzylidene]-1*H*-inden-1-one with some alkyl halides. Biological tests demonstrated that most of the synthesized compounds have moderate to good inhibitory activities effect on cholinesterase enzymes. Among them, **10e** showed the best profile as a selected compound for inhibition of hAChE (IC50 = 0.32) and hBuChE (IC50 = 0.43 μM) enzymes. Kinetic analysis and molecular docking led to a better understanding of this compound. Kinetic studies disclosed that **10e** inhibited acetylcholinesterase in mixed-type and butyrylcholinesterase in non-competitive type. The toxicity results showed that **10e** is less toxic than donepezil and has better inhibitory activity against hBuChE when compared to donepezil or Galantamine. Other performed experiments revealed that **10e** has an anti-β amyloid effect which is capable of reducing ROS, LDH and MDA also possing positive effect on TAC. On the other hand, it has shown a good anti-inflammation effect.

1. Introduction

Alzheimer's disease (AD) is a multifactorial mental disorder and one of the most common health issues which increasingly occurred in developed countries with enhancing of the elderly population. Indeed, AD is the most common type of dementia due to the defective central nervous system (CNS). AD begins with short-term memory loss and characterized by a progressive decrease or loss of memory, cognitive activities and severe behavioral such as irritability, anxiety, and depression [1–9]. Unfortunately, with an increase in life expectancy around the world, the number of people with AD is growing and expected to be several multiplies until 2050 [10,11]. Several factors can affect AD patients, including genetic, pathological changes and dysfunction of neuro-cholinergic system, the amplitude of unusual deposits of β-amyloid (Aβ) peptide, hyperphosphorylated tau protein, dyshomeostasis of biometals, neuroinflammation, and oxidative stress [12–15]. The definitive therapeutic of AD is unknown and finding a way to treat the disease has become a challenge. One of the most popular treatments existing is based on the cholinergic hypothesis by maintaining acetylcholine (ACh) levels [16–19]. Also, other futuristic treatments for AD include antioxidants, anti-inflammatory medicines, anti-amyloid strategies, and hormones [20].

In the regulation of neurotransmitter ACh in the synapse of the nervous system of the body, an enzyme interferes under the name of acetylcholinesterase (AChE) playing an important role in the hydrolysis of Ach [21–24].

The most important drugs used today to treat AD are AChE inhibitors, Donepezil, rivastigmine, galanthamine and tacrine [25,26]. Butyrylcholinesterase (BuChE) is another cholinesterase enzyme, which plays a small role in the healthy brain for ACh hydrolysis, but high levels of BuChE are found in AD patients acting as ACh hydrolyzer in the absence of AChE. Inhibition of BuChE can increase the cholinergic transmission in AD. Therefore, simultaneous inhibition of AChE and BuChE enzymes can be a beneficial treatment approach for AD [27–31].

* Corresponding author.
E-mail address: teymouri@tabrizu.ac.ir (R. Teimuri-Mofrad).

https://doi.org/10.1016/j.ejmech.2020.112140
0223-5234/

Among existing medications, donepezil was introduced as non-toxicity, blood-brain barrier permeable, reversible and non-competitive inhibitor of AChE in the USA for treatment of mild, moderate, and severe AD [32–34]. Donepezil is one of the 1-indanone analogus. 1-Indanone frameworks are available extensively in natural and biologically synthetic compounds. Among its biological activities are smooth muscle relaxant, anticancer, anti-inflammatory activity, and acetylcholinesterase (AChE) inhibition. Therefore, this combination has attracted the attention of chemists and pharmacologists [35–38].

Piperazine and its derivatives are important heterocyclic and pharmacophores compounds. They exhibit many biological activities such as anti-cancer, antipsychotic, antioxidant, anti-angina, antihistamine, anxiolytic, anti-microbial, anti-depressant, anti-fungal and anti-HIV protease activity and found in the structure of many medicines available in the market. They are also used in making the central nervous system (CNS) active agents [39–43].

In this work, we tried to design and synthesize hybrid compounds containing 2,3-dihydro-5,6-dimethoxy-1*H*-inden-1-one (a key moiety of donepezil) and a piperazinium salt as new cholinesterase enzyme inhibitors with simultaneous AChE and BuChE inhibitory activities (Fig. 1). Their effects on inhibition of AChE and BuChE enzymes were studied. The most important goal in this study was to synthesize compounds that could dual inhibition of AChE and BuChE enzymes. The conversion of neutral nitrogen in the parent compound **8** to the positive nitrogen in the ultimate compounds resulted in an increase in the anti-AChE and anti-BuChE activity. The structure of the synthesized compounds suggests that they are capable of acting as a radical scavenger possessing the ability to trap radical oxygenated species (ROS). Among the synthesized compounds, 2,3-dihydro-5,6-dimethoxy-2-[4-(4-(3-chlorobenzyl)-4-methylpiperazinium-1-yl)benzylidine]-1*H*-inden-1-one bromide (**10e**) was selected as the strongest inhibitor of AChE and BuChE enzymes for further experiments that were designed to analyze its various capabilities.

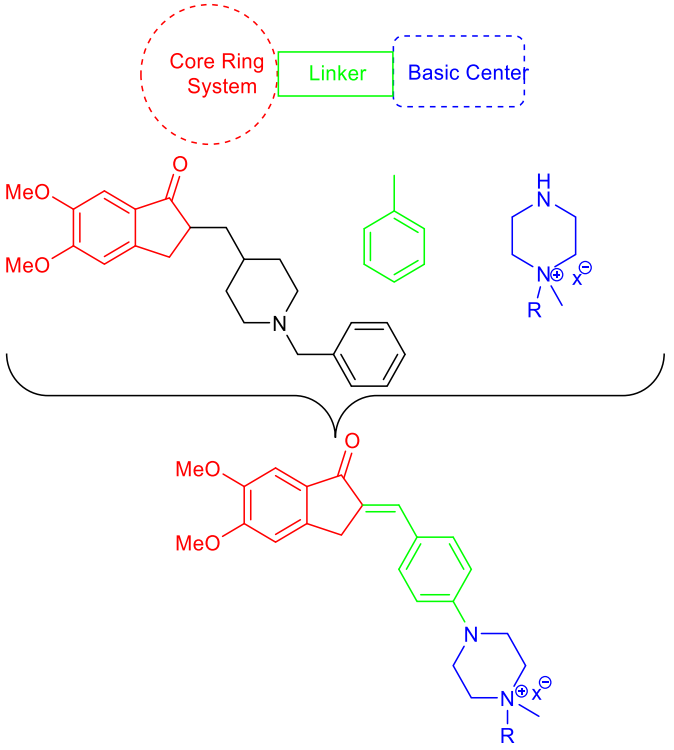

Fig. 1. Requirements in designing the structure of compounds **10a-o**.

2. Results and discussion

2.1. Chemistry

The synthetic route to the new 2,3-dihydro-5,6-dimethoxy-1*H*-inden-1-one and piperazinium salt hybrid compounds is represented in schemes 1 and 2. Target compounds were prepared by changing the functional group attached to the methylated nitrogen of piperazine and act as the inhibitor of acetylcholinesterase (AChE) and butyrylcholinesterase (BuChE) enzymes. Initially, 4-fluorobenzaldehyde (**1**) was reacted with 1-methylpiperazine (**2**) in the presence of HDTMAB and K_2CO_3 in DMF at 100 °C resulting in the formation of 4-(4-methylpiperazin-1-yl)benzaldehyde (**3**) in the yield of 49% (Scheme 1) [44]. 4-(Bromoalkoxy)benzaldehydes derivatives **6a-b** were obtained from the reaction of 4-hydroxybenzaldehyde (**4**) with appropriated dibromoalkane derivatives **5a-b** in the presence of K_2CO_3 in acetone at 56 °C, in 55 and 48% yields, respectively (Scheme 1) [45].

In the following, from the Aldol condensation reaction of 2,3-dihydro-5,6-dimethoxy-1*H*-inden-1-one (**7**) with compounds **3** and **6a-b** in the presence of NaOH 10% in EtOH at ambient temperature, 2,3-dihydro-5,6-dimethoxy-2-[4-(4-methylpiperazin-1-yl)benzylidene]-1*H*-inden-1-one (**8**) and 2,3-dihydro-5,6-dimethoxy-2-[4-(bromoalkoxy)benzylidene]-1*H*-inden-1-ones (**9a-b**) were obtained in 92, 86 and 82% yields, respectively (Scheme 2) [46,47].

The final products compounds **10a-m** were synthesized via N-alkylation reaction of compound **8** with various alkyl halides (R-X) in the presence of KI in acetonitrile at 80 °C, in good yields (Scheme 2) Compounds **10n** and **10o** with the simultaneous presence of two 1-indanone moieties in their structure were synthesized by the reaction of compound **8** with **6a** or **6b** in the presence of KI in acetonitrile at 80 °C with 55 and 50% yields, respectively (Scheme 2) [1,48].

2.2. In vitro inhibition studies of hAChE/hBuChE

The AChE and BuChE enzymes are known to be involved in AD and compounds with inhibition of both AChE and BuChE are used

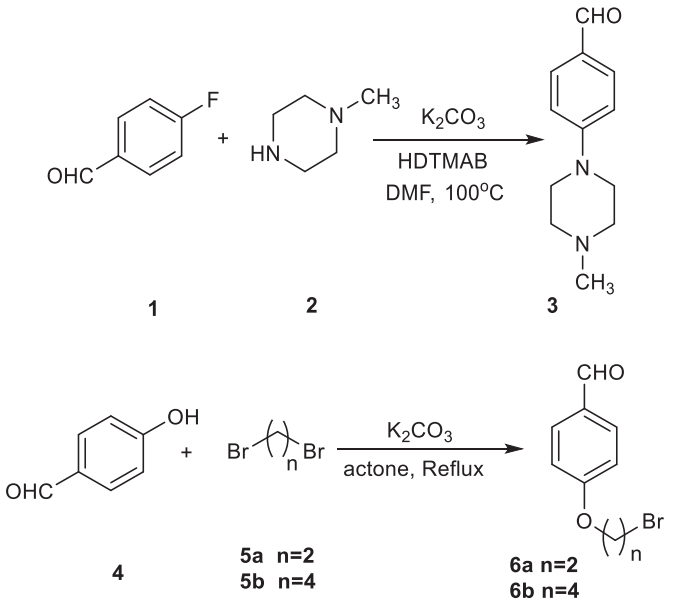

Scheme 1. Synthesis of 4-(4-methylpiperazin-1-yl)benzaldehyde (**3**) and 4-(bromoalkoxy)benzaldehydes (**6a-b**).

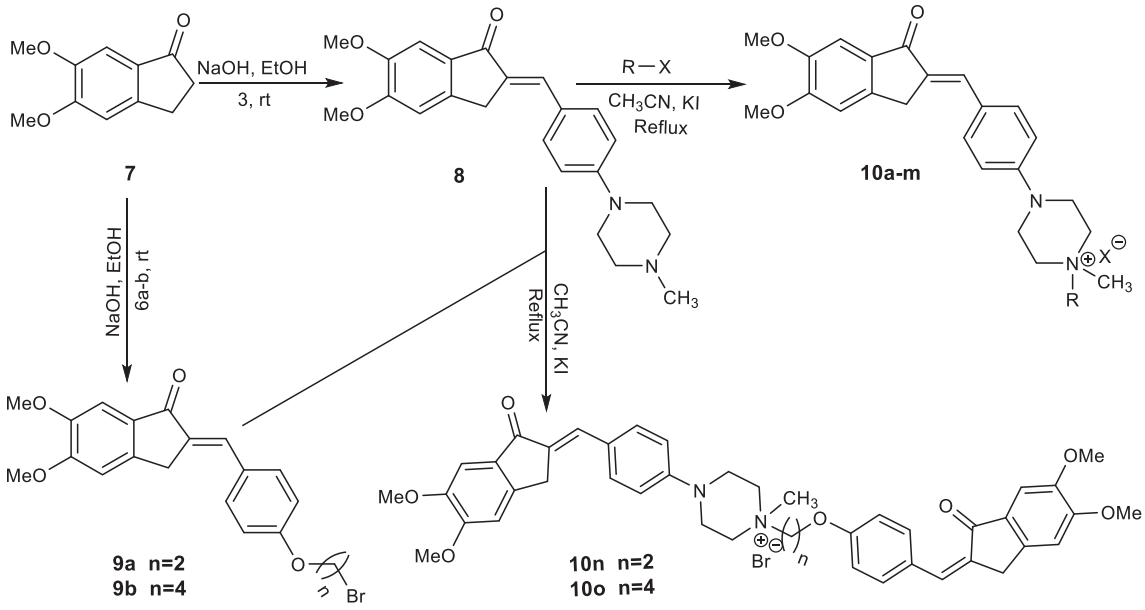

Scheme 2. Synthesis of compounds **8**, **9a-b** and 2,3-dihydro-5,6-dimethoxy-2-[4-(4-alkyl-4-methylpiperazinium-1-yl)benzylidine]-1*H*-inden-1-one halide salt derivatives (**10a-o**) as novel donepezil hybrid analogs.

for the treatment of AD. The value of inhibition of both AChE and BuChE enzymes of newly synthesized compounds **10a-o** were investigated using Ellman's spectrophotometric method [49] and the enzymes obtained from human blood. Donepezil and galantamin are used as a reference and the results are summarized in Table 1. Most of the synthesized derivatives exhibit inhibitory activity against both hAChE and hBuChE, IC_{50} values obtained for hAChE and hBuChE are between 0.32 to 12.91 μM and 0.43−25.2 μM, respectively. Compound **8** which is considered as the synthesized precursor has shown good inhibitory effects against hAChE (IC_{50} = 0.32 μM), while it does not show any significant effect on hBuChE.

However, newly synthesized compounds **10a-o** have shown moderate effect on the inhibitory activity of enzymes hAChE and hBuChE, compounds **10a** and **10e** showed simultaneous good inhibitory effects on their activity. Compound **10a** showed the hAChE inhibitory activity (IC_{50} = 0.37 μM) lower than that of donepezil while its inhibitory activity against hBuChE (IC_{50} = 0.43 μM) was higher than donepezil. Both hAChE and hBuChE inhibitory activity in compound **10a** are better than the activity in Galantamin. Compound **10e** showed hAChE inhibitory activity (IC_{50} = 0.32 μM) lower than of donepezil's and higher than of Galantamin's but in comparison to donepezil and Galantamin it possesses a better inhibitory activity against hBuChE (IC_{50} = 0.43 μM).

The presence of a positive charge within the piperazinium compounds **10** is expected not only increases interactions on the active sites of the enzymes but also to entails a "locked-in" effect in

Table 1
In vitro hAChE and hBuChE inhibitory activity of the synthesized compounds.

Compound	R-	X	IC_{50} (μM) hAChE	IC_{50} (μM) hBuChE	hAChE/hBuChE
8	–	–	0.32 ± 0.012	23.87%[a]	–
9a	–	–	6.162%[a]	5.16%[a]	–
9b	–	–	27.83%[a]	0%[a]	–
10a	$PhCH_2$-	Cl	0.37 ± 0.012	0.43 ± 0.021	0.86
10b	4-$BrPhCH_2$-	Br	2.55 ± 0.062	4.6 ± 0.13	0.55
10c	3-$BrPhCH_2$-	Br	1.99 ± 0.051	0.65 ± 0.063	3.06
10d	2-$BrPhCH_2$-	Br	0.54 ± 0.025	1.4 ± 0.071	0.38
10e	3-$ClPhCH_2$-	Br	0.32 ± 0.011	0.43 ± 0.022	0.74
10f	2-$ClPhCH_2$-	Cl	0.48 ± 0.021	2.16 ± 0.081	0.22
10g	Py-2-yl−CH_2−	Cl	0.38 ± 0.012	3.24 ± 0.12	0.12
10h	$CH_3CH_2CH_2$-	Br	2.15 ± 0.061	20.16 ± 2.1	0.11
10i	$CH_3(CH_2)_2CH_2$-	Br	0.54 ± 0.024	21.6 ± 2.3	0.02
10j	$CH_3(CH_2)_3CH_2$-	Br	0.54 ± 0.03	3.24 ± 0.1	0.17
10k	$CH_3(CH_2)_4CH_2$-	Br	4.25 ± 0.12	3.6 ± 0.12	1.18
10l	CH_2=$CHCH_2$-	Cl	0.43 ± 0.025	25.2 ± 2.3	0.02
10m	$HOCH_2CH_2$-	Cl	1.1 ± 0.041	6.48 ± 0.2	0.17
10n	$(C_{19}H_{17}O_4)CH_2$-[b]	Br	24 ± 0.02	20 ± 0.01	1.2
10o	$(C_{21}H_{21}O_4)CH_2$-[c]	Br	0	0.83 ± 0.04	–
Donepezil	–	–	0.014 ± 0.0012	14.4 ± 15	0.001
Galantamin	–	–	3 ± 0.18	31.6 ± 3	0.095

[a] Percent inhibition at a concentration of 100 μM.
[b] Resulting from compound **9a**.
[c] Resulting from compound **9b**.

the brain thus preventing peripheral cholinergic adverse effects together with enabling prolonged duration of AChEIs action in brain tissues [1,26].

1-Indanone moiety as a key part of the donepezil structure has biological activity. To go on with this study compounds **10n** and **10o** with the simultaneous presence of two 1-indanone moieties were synthesized and were expected to have good inhibitory activity. But results from biological testing as shown in Table 1 revealed that mentioned compounds had only little effect on increasing inhibitory activity than the most synthesized hybrid compounds and were not suitable alternatives for this purpose.

2.3. Kinetic study of hAChE and hBuChE inhibitions of compounds *10a* and *10e*

Toward a better understanding of the inhibition mechanism, kinetic studies of compounds **10a** and **10e** as the strongest hAChE and hBuChE inhibitors between other synthesized compounds were performed (Fig. 2). In this study, a similar mode of action was expected due to the structural similarity of these compounds. The type of inhibition was determined from the analysis of the Lineweaver–Burk plots. This pattern indicates non-competitive inhibition for compound **10a** with Ki values 0.5 μM and 0.4 μM for hAChE and hBuChE inhibitions, respectively. **10e** has the non-competitive inhibition for hBuChE with the Ki value of 0.5 μM while hAChE inhibition of this compound displayed mixed-type inhibition with 1 μM and 0.5 μM Ki and KI values, respectively (Table 2). As previously reported, compounds with the non-competitive type of inhibition, interact with enzyme PAS and mixed-type inhibition is the result of interaction with both active sites (PAS and CAS) of the enzyme [32,39].

2.4. In vitro study of the toxicity profile of compound *10a* and *10e*

Cytotoxicity of compounds **10a** and **10e** were evaluated in human foreskin fibroblast (HFF) cells, MCF-7 cells, and neuronal SH-SY5Y cells. The MTT test was used to obtain the IC_{50} values (compound concentration resulting in 50% inhibition of cell viability) after 48 h treatment of HFF, MCF-7 and SH-SY5Y cells. The results are summarized in Table 3. Donepezil has also been used as a control of these cells. IC_{50} values of **10a** and **10e** in all three studied cell lines were higher than that of donepezil which indicates that these compounds are less toxic than donepezil.

Table 2
Kinetic of hAChE and hBuChE inhibition for the compounds **10a** and **10e**.

Compounds	hAChE		hBuChE	
	Ki (μM)	KI (μM)	Ki (μM)	KI (μM)
10a	0.5	0.5	0.4	0.4
10e	1	0.5	0.5	0.5

Table 3
In vitro cytotoxicity of compounds **10a** and **10e**.

Compound	Cytotoxicity (IC_{50}, μM)		
	MCF-7	SH-SY5Y	HFF
10a	1.195	1.285	2.404
10e	1.515	1.231	1.977
Donepezil	0.060	0.300	0.091

2.5. Effect of *10e* on the protection of PC12 against Aβ (1-42) toxicity

One of the key factors that play an important role in AD is the formation of toxic aggregates of Aβ. Aβ peptides have two main isoforms including Aβ (1-40) and Aβ (1-42). The advanced accumulation of Aβ causes oxidative stress and inflammation. Thus the inhibitors of the Aβ aggregation are known as the main therapeutic strategy for AD [21,32]. Therefore, to complement the results and explore the effect of the synthesized compounds on inhibition of Aβ (1-42) aggregation, the most promising compound **10e** was examined by transmission electron microscopy (Fig. 3).

PC12 pheochromocytoma cells were selected because the cells are vulnerable to Aβ insult and have been used mostly to study β-amyloid peptide neurotoxicity [50]. The Aβ-induced PC12 cells were incubated with different concentrations of **10e**. According to the MTT result, the PC12 cells were incubated with Aβ (1-42) with or without concentration-dependent of compound **10e**. Transmission electron microscopy analysis was used for cell viability comparison. As shown in Fig. 3, Aβ-treated cells (Fig. 3b) experience

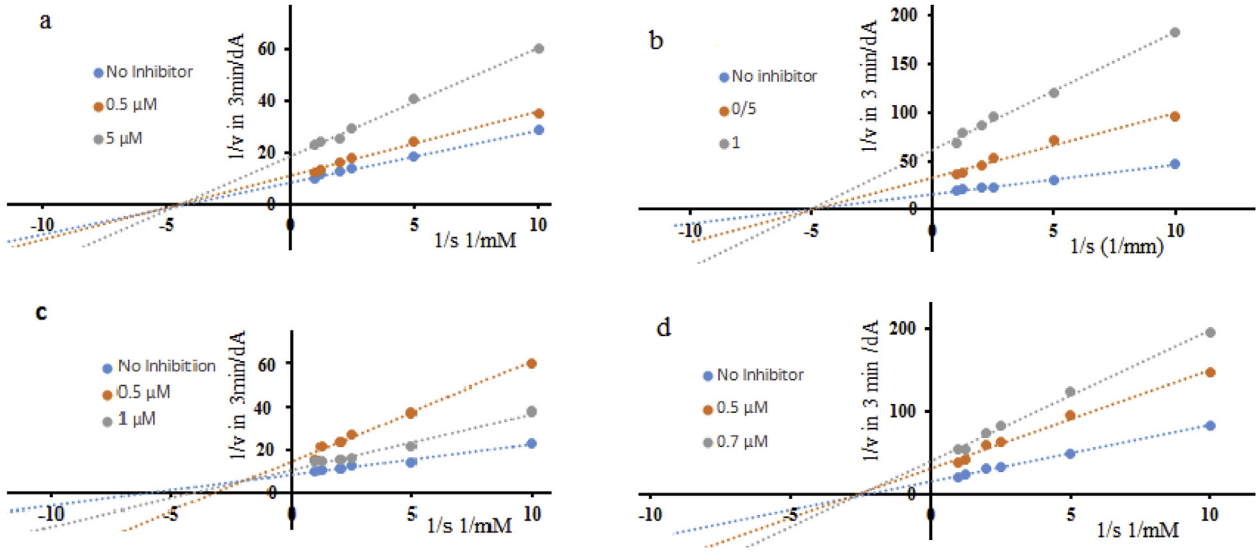

Fig. 2. Lineweaver–Burk plots of *h*AChE and hBuChE inhibition kinetics of the compounds **10a** and **10e**, (a) **10a** hAChE inhibitory (b) **10a** hBuchE inhibitory (c) **10e** hAChE inhibitory (d) **10a** hBuchE inhibitory.

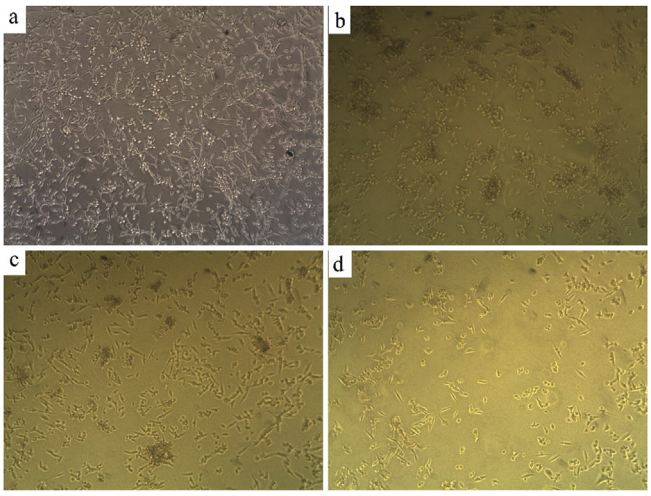

Fig. 3. Transmission electron microscopy analysis of viability of PC12 cells were incubated with and without Aβ and **10e** at 37 °C for 24 h, (a) normal PC12 cells before treatment, (b) PC12 cells incubated with Aβ (1–42) (5 ìM), (c) the Aβ-induced PC12 cells were incubated with compound **10e** (1 μM) (d) the Aβ -induced PC12 cells were incubated with compound **10e** (10 μM).

reduced cell viability when compared to control cells (Fig. 3a). The obtained TEM results offered that **10e** inhibits Aβ aggregation markedly through direct interaction. It is demonstrated that the pretreatment of cells with synthetic compound **10e** (1 μM and 10 μM) can protect them against Aβ induced cell death in a concentration-dependent manner (Fig. 3c and d, respectively).

2.6. Effect of ***10e*** on ROS levels

Previous studies suggested that oxidative injuries have an important role in AD [32,51]. One of the symptoms of heightened oxidative stress in various pathological conditions is increased levels of reactive oxygen species (ROS). Aβ (1-42) is known to stimulate oxidative stress in the pathogenesis of AD. Thus, we can predict that Aβ (1-42) leads to ROS formation the oxidation of neuronal proteins [21,52]. The anti-oxidant potential of the most potent test compound **10e**, was measured by appraising intracellular levels of ROS in the cells affected by Aβ (1-42) using 4′,6-diamidino-2-phenylindole (DAPI), deoxynucleotidyltransferase (TUNEL) and 2′,7′-dichlorofluorescine diacetate (DCFH-DA) assay. DNA with DAPI and in the TUNEL method creates a highly fluorescent complex in which the fluorescent intensity increased in the presence of ROS. After passing the cell membrane, DCFH-DA undergoes hydrolyzation by intracellular esterases to nonfluorescent DCFH. DCFH is oxidized to the fluorescent 2′,7′-dichlorofluorescine (DCF) in the presence of ROS (Fig. 4). As shown in Fig. 4, the PC12 cells display low levels of ROS while significantly increases of ROS levels were seen in the PC12 cells incubated with 5 μM of Aβ

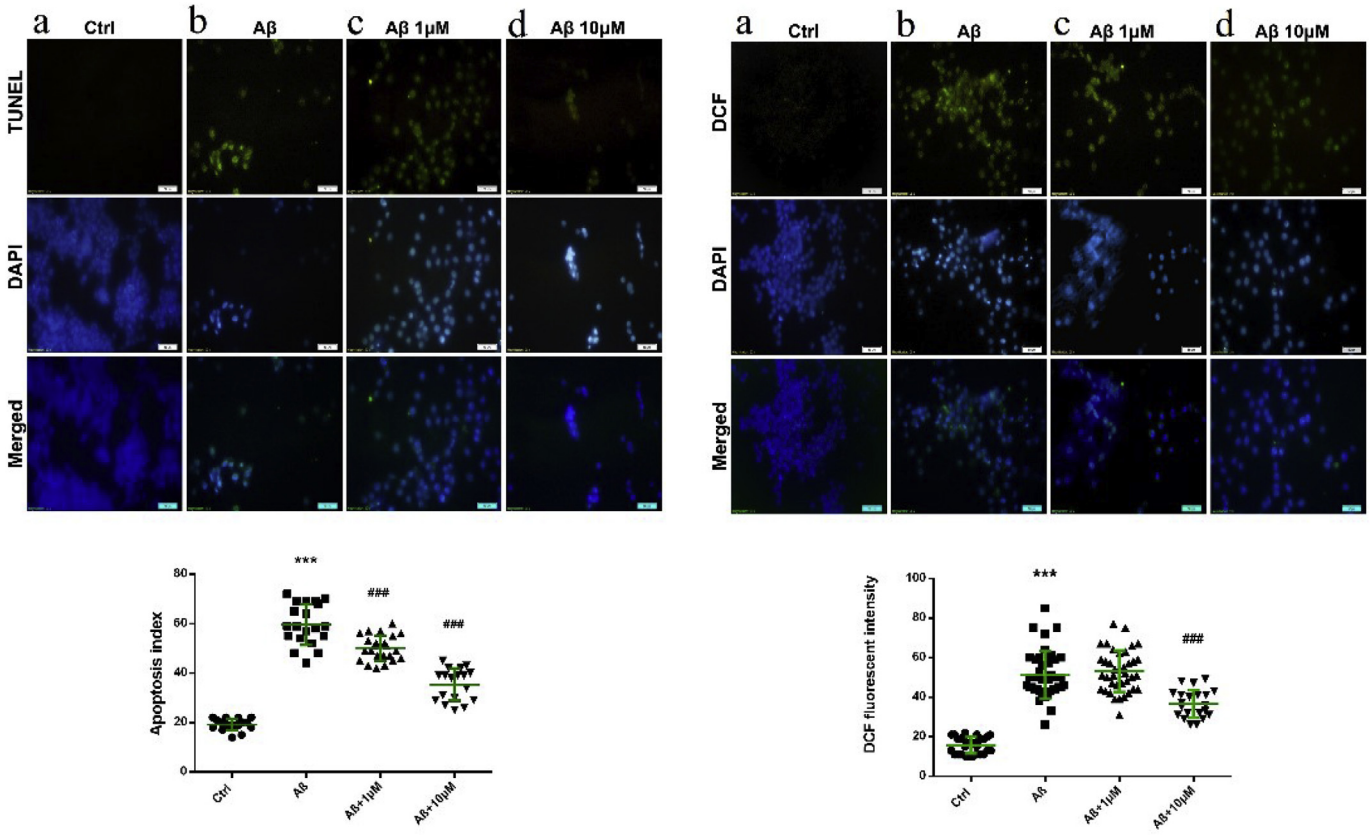

Fig. 4. Inhibition of ROS formation by **10e**, detected by the conversion of 4′,6-diamidino-2-phenylindole (DAPI), deoxynucleotidyltransferase (TUNEL) and 2′,7′-dichlorofluorescine diacetate (DCFH-DA) assay. Using a fluorescence confocal microscope helped to take color images, (a) control cells showing low levels of fluorescence (b) PC12 cells treated with 5 μM Aβ (1-42) for 48 h showing increase in ROS (c–d) reduction of ROS in Aβ (1–42)-induced toxicity treated with 1 μM and 10 μM of **10e**. (For interpretation of the references to color in this figure legend, the reader is referred to the Web version of this article.)

Table 4
Action of **10e** on the ROS formation in Aβ (1–42)-induced toxicity cells.

10e (μM)	ROS	
	Apoptosis	DCF
Control	20 ± 1	18 ± 2
Aβ 5 μM	60 ± 10	51 ± 11
1 μM	50 ± 3	51 ± 11
10 μM	35 ± 5	38 ± 4

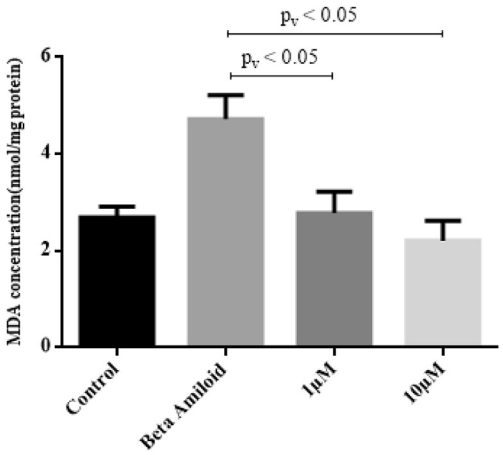

Fig. 5. MDA formation in Aβ (1-42) (5 μM)-induced toxicity in PC12 cells co-incubated with or without **10e** (1 μM and 10 μM).

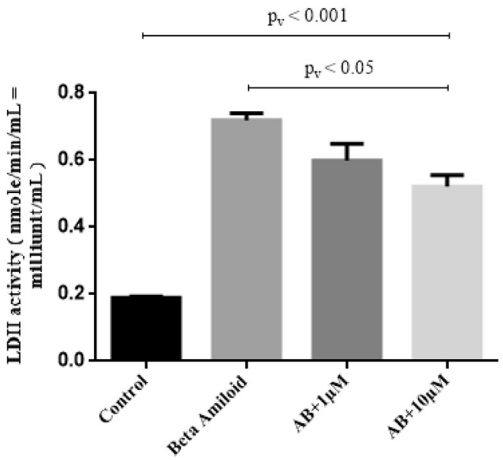

Fig. 6. LDH release in Aβ (1–42)-induced toxicity cells with and without **10e**.

(1-42) for 48 h. On the other hand, ROS formation decreases in the PC12 cells incubated with the same concentration of Aβ (1-42) in the presence of compound **10e** as a free radical scavenger. As shown in Table 4, the ROS formation in Aβ (1–42)-induced toxicity cells is three times as much as that of PC12 normal cells and the results showed that compound **10e** at 1 μM and 10 μM was able to reduce this effect in a concentration-dependent manner.

2.7. Lipid peroxidation inhibitory effect of *10e*

Malonyldialdehyde (MDA) is one of the main intermediates made during lipid peroxidation. MDA assay in biological sample supplies a simple, reproducible, and standardized tool for evaluation of lipid peroxidation. The MDA-TBA adduct formed by the

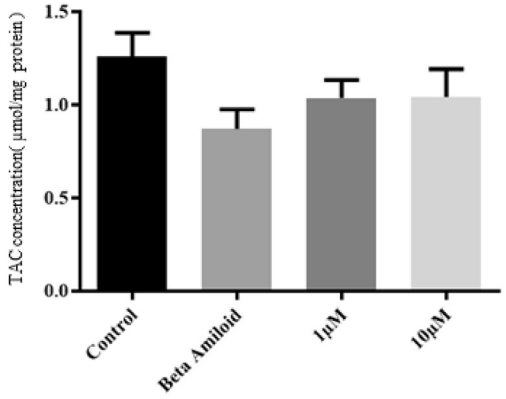

Fig. 7. Effect of compound **10e** on antioxidant capacity, in PC12 cells incubated with Aβ, with and without **10e**.

reaction of MDA and TBA under high temperature. Malondialdehyde is measured in acidic media and heat (90–100 °C) colorimetrically at 532 nm. Aβ-induced damage could cause an increase in MDA levels [21,53]. A significant increase in MDA levels was seen in the PC12 cells incubated with Aβ (1-42) (5 μM) for 8 h compared to the control cell. As shown in Fig. 5, there are a sharp increase in the MDA concentration in Aβ (1–42)-induced toxicity cells (51.9%). The addition of compound **10e** (1 μM and 10 μM) to Aβ (1–42)-induced toxicity cells provided a notable decrease in MDA levels in a concentration-dependent manner (40.4–46.2%).

2.8. Effect of *10e* on lactate dehydrogenase (LDH)

Lactate dehydrogenase (LDH) is a rather stable enzyme and an oxidoreductase that catalyses the interconversion of pyruvate and lactate and it is used to evaluate the occurrences of damage and toxicity of tissue and cells. One of the symptoms of damage and toxicity of tissue and cells is the increased levels of LDH. In AD, the enzymatic activity increases compared to normal cells [53,54]. The enzyme activity of lactate dehydrogenase is significantly increased in Aβ (1–42)-induced toxicity cells (73.6%) when compared to normal cells (Fig. 6), suggesting that impaired function is a result of its oxidative modification by Aβ (1-42). As shown in Figure 6, 1 μM and 10 μM concentration of **10e** provided a decrease in LDH levels (16.6% and 27.5%), respectively. The concentration-dependent manner of this test confirms the effect of the compound **10e** on Aβ (1–42)-induction of toxicity.

2.9. Effect of *10e* on TAC

The studies suggested that different antioxidants have the potential in delaying the progression of AD. Compounds with inhibition capability suitable for oxidation activities that occur under the influence of atmospheric oxygen or reactive oxygen species are called antioxidants. Antioxidants defend healthy brain against oxidative damages that include antioxidant enzymes such as superoxide dismutase (SOD), catalase (CAT) and free radical scavengers such as ascorbate, vitamin E. In AD, there is a decrease in the antioxidant defense system so oxidative stress can act as a risk factor for AD [55–57]. The antioxidant activity of compound **10e** was determined by the oxygen radical absorbance capacity assay using fluorescein. As can be seen in Fig. 7, there is a sharp decrease in the antioxidant system in Aβ (1–42)-induced toxicity cells, while in the presence of compound **10e** (1 μM and 10 μM) an increase in the antioxidant activity was observed.

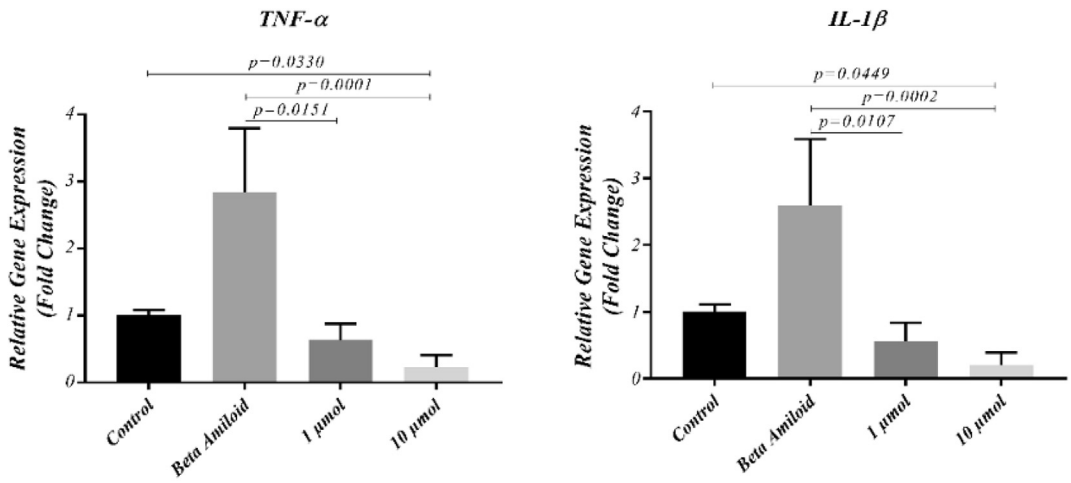

Fig. 8. Effect of **10e** on LPS-induced production of TNF-α and IL-1β by human peripheral blood monocytes.

2.10. mRNA expression levels of relevant genes

Studies show that there is an impairment in microglial function in AD in the presence of Aβ. The microglial disorder might be sustained by cytokines TNF-α and IL-1β which play an important role in the pathogenesis of inflammatory and this factor which can accelerate AD progress. Therefore, anti-inflammatory compounds of the ability to suppress TNF-α and IL-1β simultaneously are suggested as effective agents in the treatment of AD [58,59].

As shown in Fig. 8, mRNA level of IL-1β and TNF-α in Aβ treated cell line increased compared to that of the cell lines which were treated with 1 μmol and 10 μmol of **10e** peptide. Also when compared with control a decrease in the levels of these genes was observed in the cell line that treated with 10 μmol of **10e**. The exact p values of gene expression results were shown in Fig. 8 and Table 5. Gene expression results indicate a direct effect of **10e** on the reduction of inflammatory genes expression in dose dependent manner.

2.11. Molecular modeling

2.11.1. Molecular docking of compounds *10a* and *10e* with hAchE and hBuChE

Molecular docking studies on the most active compounds **10a** and **10e** were performed, to obtain more information about binding interplay with hAChEI and hBuChE in their hydrolytic active site. The results showed that the derivatives could be inhibited by binding to the active site of both cholinesterases. Docking results showed that compounds studied in the crystal structure of hAChE donepezil complex showed a similar situation to donepezil (Fig. 9) and compound **8** (Fig. 10) having good performance with acceptable binding energy. According to the results of molecular docking of compounds **10a** (Fig. 11) and **10e** (Fig. 12) in hAchE, the compound of **10a** showed a binding energy of −13.14 kcal/mol and the compound of **10e** showed a binding energy of −13.85 kcal/mol, while the binding energy relating to donepezil and compound **8** was equal to −11.71 and −11.3 kcal/mol, respectively. That low energy reflects a better interaction between the ligand and the enzyme. The methoxy group of 1-indanone moiety in the

Table 5
The exact p values of gene expression results.

Row	p TNF-α	p IL-1β
Control with 10 μM	0.0330	0.0449
Aβ with 1 μM	0.0151	0.0107
Aβ with 10 μM	0.0001	0.0002

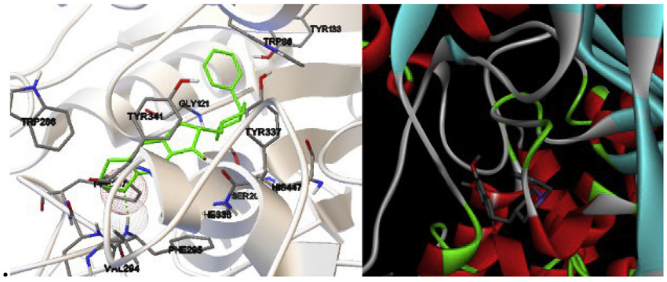

Fig. 9. Molecular docking of donepezil in hAChE active sites.

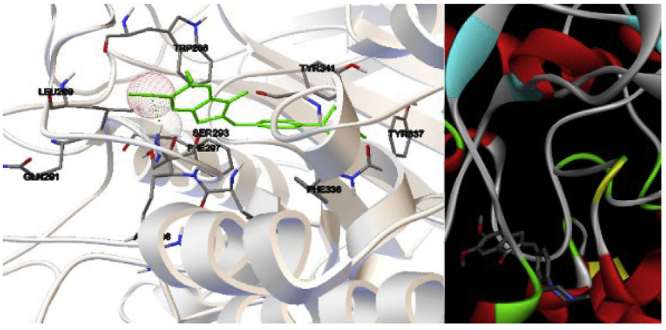

Fig. 10. Molecular docking of compound **8** in hAChE active sites.

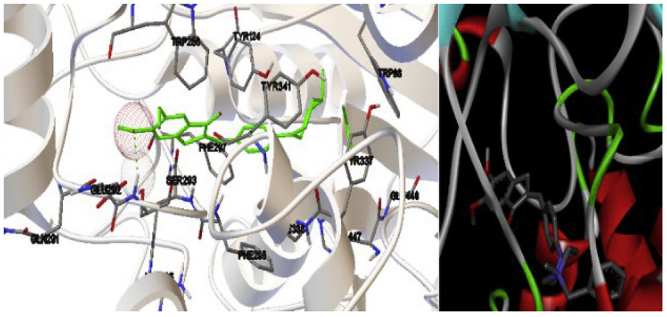

Fig. 11. Molecular docking of compounds **10a** in hAChE active sites.

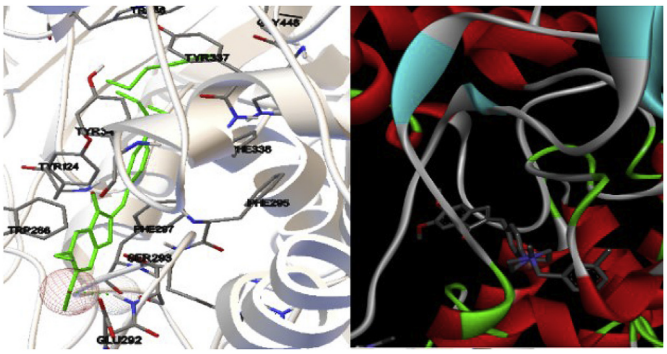

Fig. 12. Molecular docking of compounds **10e** in hAChE active sites.

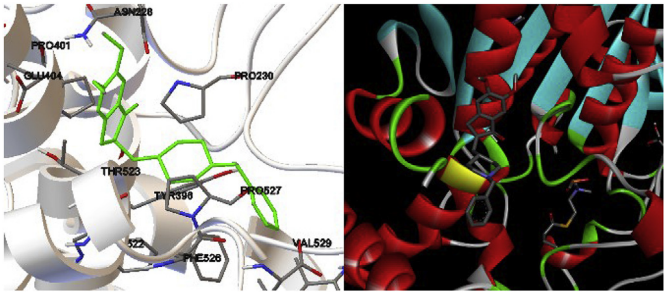

Fig. 13. Molecular docking of donepezil in hBuChE active sites.

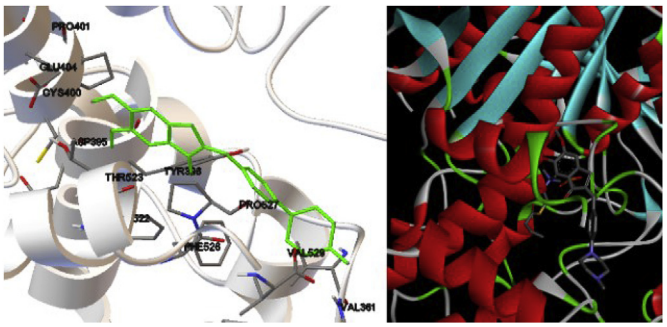

Fig. 14. Molecular docking of compounds **8** in hBuChE active sites.

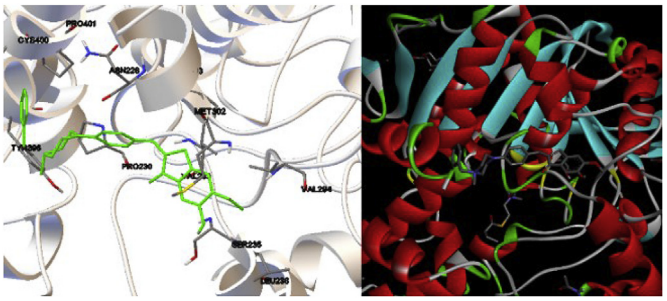

Fig. 15. Molecular docking of compounds **10a** in hBuChE active sites.

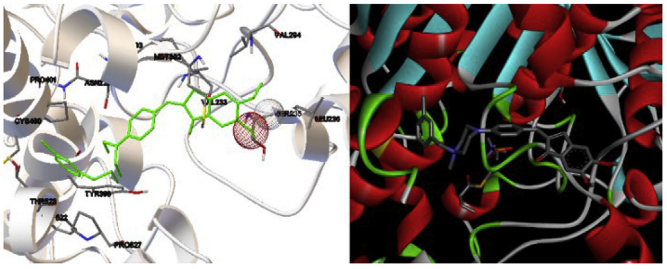

Fig. 16. Molecular docking of compounds **10e** in hBuChE active sites.

compounds **10a**, **10e** and **8** establishes *H*-bond with SER293 while this group in donepezil forms *H*-bond with PHE295. Also, according to the results obtained, compound **8** as the parent drug in this work was well fit in to the hydrophobic pocket composed of amino acids LEU289, SER293, PHE297, TRP286, TYR341, PHE338, and TYR337. Both compounds **10a** and **10e** show the same results. They also were interacted with the same amino acids as done for compound **8**, other amino acids that these compounds fit them as follows: amino acids GLU292, ARG298, TYR124 and PHE295 placing around 1-indanone and phenyl ring of benzylidine group and Amino acids TRP86, TYR341, TYR337, HIS447 and GLY448 in the catalytic anionic site (CAS) placing around piperazinium salt moiety in compounds **10a** and **10e**. The quaternary nitrogen of this piperazinium ring facilitates ligand recognition through binding to the catalytic anionic site (CAS) comprising TYR337. The phenyl ring of the benzyl group in these compounds has π-π interaction with HIS447 of CAS.

Presence of more interactions with amino acids, except for the common ones, between the parent drug and compounds **10a** and **10e**, may be a reason for better interactions of these compounds with the hAchE enzyme.

Docking results showed that compounds studied in the crystal structure of hBuChE showed a different situation to donepezil (Fig. 13) and compounds **8** (Fig. 14) having good performance with acceptable binding energy. According to the results of molecular docking of compounds **10a** (Fig. 15) and **10e** (Fig. 16) in hBuChE, the compound of **10a** showed a binding energy of −10.5 kcal/mol and the compound of **10e** showed a binding energy of −10.6 kcal/mol, while the binding energy relating to donepezil and compounds **8** was equal to −9.53 and −9.27 kcal/mol, respectively. That low energy indicates the better interaction between the ligand and the hBuChE enzyme. 1-Indanone methoxy group of compound **10e** establishes *H*-bond with Leu 236 while the compound of **10a,** donepezil and compounds **8** do not show any hydrogen bonding. Additionally, according to the results, parent compound **8** was well fit in to the hydrophobic pocket composed of amino acids PRO401, CYS400, GLU404, ASP395, THR523, TYR396, PHE526, PRO527, VAL529, and VAL361. Amino acids VAL233, SER235, PRO230, MET302, and ASN228 fit with 1-indanone and phenyl ring of benzylidine group and amino acids TYR396, TRP522 and CYS400 placed around the positive charge of piperazinium salt moiety in the compound **10a**. Docking result of compound **10e** shows that amino acids VAL233, SER235, LEU236, MET302, and ASN228 fit with 1-indanone and phenyl ring of benzylidine group and amino acids TYR396, PRO527, THR523, CYS400, PRO401, and TRP522 took place around the positive charge of piperazinium salt moiety in compound **10e**. The quaternary nitrogen of the piperazinium ring in compounds **10a** and **10e** facilitates ligand recognition through binding to the TYR396 and the phenyl ring of the benzyl group in these compounds has π-π interaction with TRP522. The difference in amino acids that parent compound **8** interacted with compared to the ones which interacted with compounds **10a** and **10e** could be a reason for better interactions observed in hBuChE enzyme.

*2.11.2. Molecular docking of compound **10e** with Aβ*

Molecular docking studies on the most active form of compound

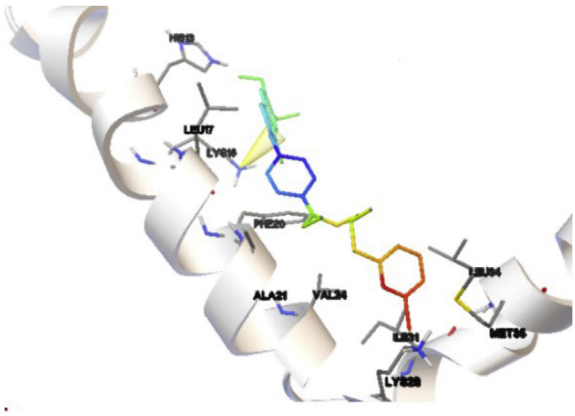

Fig. 17. Molecular docking of **10e** with Aβ peptide active sites.

10e was performed to understand the binding mode and the interaction of the compound with Aβ (1-42). The results showed that this compound binds with Aβ (1-42). Compound **10e** is transversely fitted along the major helix. The results of molecular docking for compound **10e** (Fig. 17) in Aβ, showed binding energy of −6.34 kcal/mol. Compound **10e** did not show any hydrogen bonding. 1-Indanone and phenyl ring of compound **10a**, showed hydrophobic interactions with residues HIS13, LEU17, LYS16, and PHE20 and the positive charge of piperazinium salt moiety in compound **10e** have interaction with residues ALA21, VAL24, LYS28, ILE31, LEU34, and MET31.

3. Conclusion

In summary, several novel 2,3-dihydro-5,6-dimethoxyinden 2-[4-(4-alkyl-4-methyl-piperazinium-1-yl)benzylidene)-1*H*-inden-1-one halides containing the 1-indanone moiety of donepezil and piperazine ring were designed, synthesized and tested for their biological activities on AD. Most of the compounds exhibited a good inhibitory effect on AChE and BuChE, among them compounds **10a** and **10e** displayed more inhibition activity. The preliminary structure-activity relationships, molecular modeling, and Kinetic study gave us valuable insight to understand the interactions between the enzyme and its ligand. Other biological tests of **10e** such as ROS, LDH, MDA, and TAC confirmed that this compound has the potent antioxidant and anti-inflammatory activities suggesting compound **10e** to be beneficial for AD treatment. Alzheimer's is a multifactorial disease and could benefited from the development of multifunctional compounds for curing AD which act on different pathways simultaneously. Findings in the present study could be taken in to consideration as a way for the progress of drug development in AD treatment. By being capable to be carried out more in vitro and *in vivo* tests include, inhibition investigation on Monoamine oxidase (MAO), beta-amyloid peptide aggregation and tau protein aggregation and measurement of the blood-brain-barrier permeability and using liposomal carriers on the mentioned compounds here. Also a notable result compound **8** can be potentially used in the designing other hybrid drugs for Alzheimer's disease.

4. Experimental section

4.1. Materials and instruments

All materials purchased from Merck and Sigma-Aldrich and used without any further purification. Solvents were dried with an appropriate dryer. Column chromatography was carried out by using Silica gel 60 (Merck, Germany). TLC plates were visualized using on UV light at 254 nm. Nuclear Magnetic Resonance spectra for ^{1}H NMR (400 MHz) and ^{13}C NMR (100 MHz) were recorded by using Bruker FT-400 spectrometer. $CDCl_3$ or DMSO-d_6 were used as solvent and chemical shifts were reported in δ values (ppm) relative to internal Me_4Si and *J* values were reported in Hz. S, singlet; d, doublet; t, triplet; q, quarted; dd, doublet of doublet; br, broad; m, mutiplet were used for peak multiplicities as abbreviations. FT-IR spectra were recorded by the Bruker Tensor 27 instrument in/on KBr plate. The melting points were measured with an electro-thermal apparatus MEL-TEMP model 1202 with open capillaries. Elemental analysis was performed on an Elemen-tar Vario EL III instrument.

4.2. Synthesis of 4-(4-methylpiperazin-1-yl)benzaldehyde (3) [44]

The mixture of 4-fluorobenzaldehyde (**2**) (3 g, 24.19 mmol), 1-methylpiperazine (**1**) (4.83 g, 48.38 mmol), HDTMAB (3.49 g, 9.6 mmol) and K_2CO_3 (6.67 g, 48.38 mmol) in DMF (12 ml) was stirred for 5.5 h at 100 °C. The reaction mixture was diluted with water and was extracted with dichloromethane (3 × 10 ml) and the organic layer was washed with water and brine, dried over sodium sulfate and the solvent was evaporated using rotary evaporator. The obtained yellow oil was purified on silica gel column chromatography with hexane/ethyl acetate (4:6) as eluent. The yellow powder (2.4 g, 11.76 mmol) of compound 3 was obtained as the desired product (49% yield).

4.3. General procedure for the synthesis of compounds 6a-b [45]

Compounds **6a-b** were synthesized as previously described in the literature [45]. Potassium carbonate (3.89 g, 28.2 mmol) was added to a solution of 4-hydroxybenzaldehyde (**4**) (3.52 g, 28.9 mmol) in 20 ml dry acetone and the mixture was refluxed for 24 h. In a two-necked flask equipped with a condenser and additional funnel was added dibromoalkane (98.6 mmol) and 20 ml acetone. Then the mixture of 4-hydroxybenzaldehyde (**4**) and potassium carbonate in acetone mixture was added drop-wise with stirring to the flask by additional funnel. The resulting solution was heated to reflux under stirring for 72 h. Acetone was evaporated using rotary evaporator apparatus. The mixture was extracted with dichloromethane (3 × 20 ml) and the combined organic layer was washed with water and brine, dried over anhydrous Na_2SO_4 and then dichloromethane was evaporated using rotary evaporator. The residue was purified on silica gel column chromatography with hexane/ethyl acetate (8:2) as eluent.

4.3.1. 4-(2-Bromoethoxy)benzaldehyde (6a)

From 8.5 ml (98.6 mmol) of 1,2-dibromoethane as reactant; 3.58 g (15.6 mmol) of white solid was obtained (55% yield, mp. 40−45 °C).

4.3.2. 4-(4-Bromobutoxy)benzaldehyde (6b)

From 11.67 ml (98.6 mmol) of 1,4-dibromobutane as reactant; 3.50 g (13.62 mmol) of white paste was obtained (48% yield).

4.4. General procedure for the synthesis of compounds 8 and 9a-b [45,47]

2,3-Dihydro-5,6-dimethoxy-1*H*-inden-1-one (7) (1 g, 5.2 mmol) and benzaldehyde derivatives **3** or **6a-b** (5.2 mmol) were dissolved in ethanol (30 ml). Aqueous NaOH solution (10% W/W, 10 ml) was added to this solution dropwise with stirring. The reaction mixture was stirred for 48 h at room temperature. The precipitate was

filtered and washed with aqueous ethanol solution (50% V/V) and then the solid product was dried under vacuum and used without further purification.

4.4.1. 2,3-Dihydro-5,6-dimethoxy-2-[4-(4-methylpiperazin-1-yl) benzylidene]-1H-inden-1-one (**8**)

From 1.06 g of compound **3** as reactant, 1.81 g (4.8 mmol) of yellow solid was obtained (92% yield); mp. 220–222 °C; FT-IR (KBr): ν 2925 (C–H), 2862 (C–H), 1684 (C=O), 1610–1510 (C=C), 1312 (C–N), 1127 (C–O) cm^{-1}; ^1H NMR (400 MHz, $CDCl_3$): δ 2.39 (3H, s, C**H**$_3$), 2.63 (4H, t, J = 8 Hz, N–C**H**), 3.36 (4H, t, J = 8 Hz, N–C**H**), 3.87 (2H, s, C**H**$_2$), 3.94 (3H, s, O–C**H**$_3$), 3.98 (3H, s, O–C**H**$_3$), 6.87 (2H, d, J = 8.7 Hz, Ar–**H**), 6.92 (1H, s, Ar–**H**), 7.27 (1H, s, Ar–**H**), 7.47 (1H, s, =C**H**), 7.52 (2H, d, J = 8.7 Hz, Ar–**H**) ppm; ^{13}C NMR (100 MHz, $CDCl_3$): δ 31.0, 55.1, 55.2, 103.9, 106.0, 109.4, 119.7, 122.0, 122.8, 129.5, 129.8, 130.9, 132.2, 134.1, 135.3, 135.6, 140.9, 143.1, 143.6, 148.6, 154.5, 191.7 ppm. Anal. Calcd. For $C_{23}H_{26}N_2O_3$ (378.47): C 72.99, H 6.92, N 7.40; Found: C 72.85, H 6.84, N 7.47%.

4.4.2. 2,3-Dihydro-5,6-dimethoxy-2-[4-(2-bromoethoxy) benzylidene]-1H-inden-1-one (**9a**)

From 1.19 g of Compound **6a** as reactant, 1.81 g (4.5 mmol) of white solid was obtained (86% yield), mp. 170–172 °C; FT-IR (KBr): ν 3028 (C–H), 2828 (C–H), 1683 (C=O), 1597–1504 (C=C), 1254 (C–O), 540 (C–Br) cm^{-1}; ^1H NMR (400 MHz, $CDCl_3$): δ 3.66 (2H, t, J = 6.2 Hz, C**H**$_2$–Br), 3.90–3.96 (5H, m, O–C**H**$_3$ and C**H**$_2$), 3.99 (3H, s, O–C**H**$_3$), 4.34 (2H, t, J = 6.2 Hz, O–C**H**$_2$), 6.96–6.98 (3H, m, Ar–**H**), 7.33 (1H, s, =C**H**), 7.54 (1H, s, Ar–**H**), 7.60 (2H, d, J = 8.7 Hz, Ar–**H**) ppm; ^{13}C NMR (100 MHz, $CDCl_3$): δ 27.7, 31.0, 55.1, 55.2, 66.7, 103.0, 103.9, 106.0, 106.4, 113.9, 127.9, 130.1, 130.8, 131.2, 132.4, 143.6, 148.4, 154.1, 157.9, 192.1 ppm. Anal. Calcd. For $C_{20}H_{19}BrO_4$ (403.27): C 59.57, H 4.75; Found: C 59.43, H 4.70%.

4.4.3. 2,3-Dihydro-5,6-dimethoxy-2-[4-(4-bromobutoxy) benzylidene]-1H-inden-1-one (**9b**)

From 1.34 g of compound **6b** as reactant, 1.85 g (4.3 mmol) of white solid was obtained (82% yield), mp. 172–176 °C; FT-IR (KBr): ν 2937 (C–H), 2878 (C–H), 1682 (C=O), 1600–1501 (C=C), 1304–1244 (C–O), 540(C–Br) cm^{-1}; ^1H NMR (400 MHz, $CDCl_3$): δ 1.93–1.99 (2H, m, C**H**$_2$), 2.04–2.11 (2H, m, C**H**$_2$), 3.49 (2H, t, J = 6.4 Hz,C**H**$_2$–Br), 3.90 (2H, s, C**H**$_2$), 3.93 (3H, s, O–C**H**$_3$), 3.98 (3H, s, O–C**H**$_3$), 4.04 (2H, t, J = 6.0 Hz, O–C**H**$_2$), 6.92–6.96 (3H, m, Ar–**H**), 7.31 (1H, s,=C**H**), 7.53 (1H, s, Ar–**H**), 7.58 (2H, d, J = 8.7 Hz, Ar–**H**) ppm; ^{13}C NMR (100 MHz, $CDCl_3$): δ 26.7, 28.3, 31.1, 32.2, 55.1, 55.2, 65.9, 104.0, 106.1, 113.8, 127.3, 130.2, 131.1, 131.2, 132.1, 143.5, 148.5, 154.1, 158.8, 192.1 ppm. Anal. Calcd. For $C_{22}H_{23}BrO_4$ (431.33): C 61.26, H 5.37; Found: C 61.16, H 5.40%.

4.5. General procedure for the synthesis of compounds **10a-m** [1,48]

The mixture of compound **8** (0.098 g, 0.26 mmol) and appropriated alkyl halides (R-X) (0.79 mmol) in acetonitrile (5 ml) was refluxed for 24 h. The precipitate was filtered and washed with acetonitrile, and then the solid product was dried under vacuum.

4.5.1. 2,3-Dihydro-5,6-dimethoxy-2-[4-(4-benzyl-4-methylpiperazinium-1-yl)benzylidine]-1H-inden-1-one chloride (**10a**)

From 0.099 g of benzyl chloride as reactant, 0.11 g of orange solid was obtained (84% yield), mp. 188–195 °C; FT-IR (KBr): ν 2963 (C–H), 2837 (C–H), 1680 (C=O), 1596–1504 (C=C), 1306 (C–N), 1251 (C–O) cm^{-1}; ^1H NMR (400 MHz, DMSO): δ 3.08 (3H, s, C**H**$_3$), 3.50–3.54 (5H, m, N–C**H**$_2$), 3.64 (2H, s, N–C**H**$_2$), 3.79 (3H, s, O–C**H**$_3$), 3.87 (3H, s, O–C**H**$_3$), 3.91 (3H, s, C**H**$_2$, N–C**H**$_2$), 4.77 (2H, s, N–C**H**$_2$),7.10 (2H, d, J = 8.7 Hz, Ar–**H**), 7.18 (2H, d, J = 11.9 Hz, Ar–**H**), 7.34 (1H, s, =C**H**), 7.52–7.55 (3H, m, Ar–**H**), 7.63 (4H, m, Ar–**H**) ppm; ^{13}C NMR (100 MHz, DMSO): δ 31.9, 41.2, 44.9, 55.8, 56.2, 58.4, 67.2, 104.6, 108.3, 115.3, 126.2, 127.4, 129.2, 130.4, 130.6, 131.6, 132.2, 132.8, 133.4, 145.0, 149.4, 150.1, 155.2, 192.2 ppm. Anal. Calcd. For $C_{30}H_{33}ClN_2O_3$ (505.06): C 71.34, H 6.59, N 5.55; Found: C 71.41, H 6.63, N 5.48%.

4.5.2. 2,3-Dihydro-5,6-dimethoxy-2-[4-(4-(4-bromobenzyl)-methylpiperazinium-1-yl)benzylidine]-1H-inden-1-one bromide (**10b**)

From 0.197 g of 4-bromobenzyl bromide as reactant, 0.14 g of yellow solid was obtained (87% yield), mp. 210–215 °C; FT-IR (KBr): ν 2963 (C–H), 2837 (C–H), 1683 (C=O), 1597–1507 (C=C), 1306 (C–N), 1250 (C–O) cm^{-1}; ^1H NMR (400 MHz, DMSO-d_6): δ 3.08 (3H, s, C**H**$_3$), 3.47–3.54 (5H, m, N–C**H**$_2$), 3.79 (3H, s, O–C**H**$_3$), 3.87 (4H, s, O–C**H**$_3$, N–C**H**$_2$), 3.90 (3H, br, C**H**$_2$, N– C**H**$_2$), 4.76 (2H, s, N–C**H**$_2$),7.10 (2H, d, J = 8.6 Hz, Ar–**H**), 7.17 (2H, d, J = 11.0 Hz, Ar–**H**), 7.33 (1H, s, =C**H**), 7.57 (2H, d, J = 8.2 Hz, Ar–**H**), 7.64 (2H, d, J = 8.6 Hz, Ar–**H**), 7.73 (2H, d, J = 8.2 Hz, Ar–**H**) ppm; ^{13}C NMR (100 MHz, DMSO-d_6): δ 31.8, 41.1, 44.8, 55.8, 56.1, 58.4–66.2, 104.6, 108.2, 115.3, 124.5, 126.2, 126.7, 130.4, 131.5, 132.1, 132.2, 132.7, 135.4, 145.0, 149.3, 150.0,155.1, 192.2. Anal. Calcd. For: $C_{30}H_{32}Br_2N_2O_3$ (628.41); C 57.34, H 5.13, N 4.46; Found: C 57.23, H 5.09, N 4.42%.

4.5.3. 2,3-Dihydro-5,6-dimethoxy-2-[4-(4-(3-bromobenzyl)-4-methylpiperazinium-1-yl)benzylidine]-1H-inden-1-one bromide (**10c**)

From 0.197 g of 3-bromobenzyl bromide as reactant, 0.15 g of yellow solid was obtained (93% yield); mp. 209–213 °C; FT-IR (KBr): ν 2987 (C–H), 2838 (C–H), 1671 (C=O), 1582–1474 (C=C), 1303 (C–N), 1247 (C–O) cm^{-1}; ^1H NMR (400 MHz, DMSO-d_6): δ 3.13 (3H, s, C**H**$_3$), 3.51–3.56 (4H, m, N–C**H**$_2$), 3.63–3.66 (2H, m, N–C**H**$_2$), 3.82 (3H, s, O–C**H**$_3$), 3.89 (3H, s, O–C**H**$_3$), 3.93 (3H, br, C**H**$_2$, N–C**H**$_2$), 3.96 (1H, br, N–C**H**$_2$), 4.83 (2H, s, N–C**H**$_2$),7.12 (2H, d, J = 8.8 Hz, Ar–**H**), 7.19 (2H, d, J = 6.4 Hz, Ar–**H**), 7.36 (1H, s, =C**H**), 7.51 (1H, t, J = 7.8 Hz, Ar–**H**), 7.65–7.67 (3H, m, Ar–**H**), 7.77 (1H, d, J = 8.0 Hz, Ar–**H**), 7.88 (1H, br, Ar–**H**) ppm; ^{13}C NMR (100 MHz, DMSO-d_6): δ 31.6, 40.9, 44.5, 55.6, 55.9, 58.3, 65.8, 104.4, 108.0, 115.0, 122.0, 126.0, 129.9, 130.2, 131.0, 131.2, 132.0, 132.3, 132.5, 133.2, 135.5, 144.6, 149.2, 149.8, 154.9, 191.7 ppm. Anal. Calcd. For: $C_{30}H_{32}Br_2N_2O_3$ (628.41): C 57.34, H 5.13, N 4.46; Found: C 57.40, H 5.16, N 4.42%.

4.5.4. 2,3-Dihydro-5,6-dimethoxy-2-[4-(4-(2-bromobenzyl)-4-methylpiperazinium-1-yl)benzylidine]-1H-inden-1-one bromide (**10d**)

From 0.197 g of 2-bromobenzyl bromide as reactant, 0.13 g of yellow solid was obtained (81% yield); mp. 181–185 °C; FT-IR (KBr): ν 2987 (C–H), 2841 (C–H), 1675 (C=O), 1592–1503 (C=C), 1302 (C–N), 1255 (C–O) cm^{-1}; ^1H NMR (400 MHz, DMSO-d_6): δ 3.17 (3H, s, C**H**$_3$), 3.46–3.52 (2H, m, N–C**H**$_2$), 3.63–3.67 (2H, m, N–C**H**$_2$), 3.72–3.78 (2H, m, N–C**H**$_2$), 3.83 (3H, s,O–C**H**$_3$), 3.90 (3H, s,O–C**H**$_3$), 3.95 (3H, br, C**H**$_2$, N–C**H**$_2$), 3.99 (1H, br, N–C**H**$_2$), 4.88 (2H, s, N–C**H**$_2$),7.12 (2H, d, J = 8.9 Hz, Ar–**H**), 7.21 (2H, d, J = 3.4 Hz, Ar–**H**), 7.38 (1H, s, =C**H**), 7.51 (1H, td, J = 7.6, 1.6 Hz, Ar–**H**), 7.58 (1H, td, J = 7.5, 1.2 Hz, Ar–**H**), 7.67 (2H, d, J = 8.8 Hz, Ar–**H**), 7.77 (1H, dd, J = 7.6, 1.5 Hz, Ar–**H**), 7.85 (1H, dd, J = 7.9, 1.2 Hz, Ar–**H**) ppm; ^{13}C NMR (100 MHz, DMSO-d_6): δ 31.6, 40.9, 44.3, 55.6, 55.9, 58.5, 66.8, 104.5, 108.0, 115.0, 126.0, 127.0, 127.18, 128.2, 130.2, 131.2, 131.9, 132.5, 132.6, 132.8, 134.1, 136.1, 144.6, 149.2, 149.8, 154.9, 191.7 ppm. Anal. Calcd. For: $C_{30}H_{32}Br_2N_2O_3$ (628.41): C 57.34, H 5.13, N 4.46; Found: C 57.28, H 5.11, N 4.49%.

*4.5.5. 2,3-Dihydro-5,6-dimethoxy-2-[4-(4-(3-chlorobenzyl)-4-methylpiperazinium-1-yl)benzylidine]-1H-inden-1-one bromide (**10e**)*

From 0.16 g of 3-chlorobenzyl bromide as reactant, 0.13 g of orange solid was obtained (86% yield); mp. 219–224 °C; FT-IR (KBr): ν 2988 (C–H), 2944 (C–H), 1672 (C=O), 1581–1471(C=C), 1303 (C–N), 1250 (C–O) cm^{-1}; ^{1}H NMR (400 MHz, DMSO-d_6): δ 3.13 (3H, s, C**H**$_3$), 3.49–3.54 (4H, m, N–C**H**$_2$), 3.63–3.65 (2H, m, N–C**H**$_2$), 3.82 (3H, s, O–C**H**$_3$), 3.89 (3H, s, O–C**H**$_3$), 3.92–3.95 (4H, m, C**H**$_2$, N–C**H**$_2$), 4.82 (2H, s, N–C**H**$_2$),7.12 (2H, d, *J* = 8.8 Hz, Ar–**H**), 7.20 (2H, d, *J* = 7.17 Hz, Ar–**H**), 7.37 (1H, s, =C**H**), 7.57–7.68 (5H, m, Ar–**H**), 7.74 (1H, s, Ar–**H**) ppm; ^{13}C NMR (100 MHz, DMSO-d_6): δ 31.7, 40.9, 44.5, 55.6, 55.9, 58.3, 65.9, 104.4, 108.0, 115.0, 126.0, 129.7, 130.2, 130.4, 130.8, 131.2, 131.9, 132.0, 132.5, 132.8, 133.4, 144.6, 149.2, 149.9, 154.9, 191.8; Anal. Calcd. For $C_{30}H_{32}BrClN_2O_3$ (583.95): C 61.71, H 5.52, N 4.80; Found: C 61.59, H 5.48, N 4.76%.

*4.5.6. 2,3-Dihydro-5,6-dimethoxy-2-[4-(4-(2-chlorobenzyl)-4-methylpiperazinium-1-yl)benzylidine]-1H-inden-1-one chloride (**10f**)*

From 0.127 g of 2-chlorobenzyl chloride as reactant, 0.13 g of dark yellow solid was obtained (93% yield); mp. 164–169 °C; FT-IR (KBr): ν 2969 (C–H), 2836 (C–H), 1678 (C=O), 1595–1505 (C=C), 1306 (C–N), 1251(C–O) cm^{-1}; ^{1}H NMR (400 MHz, DMSO-d_6): δ 3.16 (3H, s, C**H**$_3$), 3.63–3.66 (3H, m, N–C**H**$_2$), 3.71–3.73 (2H, m, N–C**H**$_2$), 3.82 (3H, s,O–C**H**$_3$), 3.89 (3H, s,O–C**H**$_3$), 3.94 (3H, br, C**H**$_2$, N–C**H**$_2$), 3.97 (1H, br, N–C**H**$_2$), 4.90 (2H, s, N–C**H**$_2$),7.12 (2H, d, *J* = 8.8 Hz, Ar–**H**), 7.20 (2H, d, *J* = 7.9 Hz, Ar–**H**), 7.36 (1H, s, =C**H**), 7.53 (1H, td, *J* = 7.5, 1.2 Hz, Ar–**H**), 7.60 (1H, td, *J* = 8.0, 1.5 Hz, Ar–**H**), 7.65–7.69 (3H, m, Ar–**H**), 7.79 (1H, dd, *J* = 7.5, 1.2 Hz, Ar–**H**); ^{13}C NMR (100 MHz, DMSO-d_6): δ 31.7, 41.0, 44.3, 55.7, 56.0, 58.5, 64.6, 104.5, 108.2, 115.1, 125.5, 127.8, 130.7, 131.4, 132.1, 132.7, 136.1, 136.2, 144.8, 150.0, 155.0, 192.0; Anal. Calcd. For $C_{30}H_{32}Cl_2N_2O_3$ (539.50): C 66.79, H 5.98, N 5.19; Found: C 66.86, H 5.92, N 5.22%.

*4.5.7. 2,3-Dihydro-5,6-dimethoxy-2-[4-(4-((pyridine-2-yl)methyl)-4-methylpiperazinium)-1-yl)benzylidine]-1H-inden-1-one chloride (**10g**)*

From 0.1 g of 2-(chloromethyl)pyridine as reactant, 0.1 g of dark yellow solid was obtained (77% yield); mp. 210–214 °C; FT-IR (KBr): ν 2959 (C–H), 2840 (C–H), 1674 (C=O), 1595 (C=C), 1302 (C–N), 1253(C–O) cm^{-1}; ^{1}H NMR (400 MHz, DMSO-d_6): δ 3.18 (3H, s, C**H**$_3$), 3.63–3.66 (4H, m, N–C**H**$_2$), 376–378 (2H, m, N–C**H**$_2$), 3.81 (3H, s, O–C**H**$_3$), 3.85–3.87 (1H, m, N–C**H**$_2$), 3.88(3H, s, O–C**H**$_3$), 3.93 (2H, s, C**H**$_2$), 4.89 (2H, s, N–C**H**$_2$),7.12 (2H, d, *J* = 8.7 Hz, Ar–**H**), 7.19 (2H, d, *J* = 9.2 Hz, Ar–**H**), 7.36 (1H, s, =C**H**), 7.54–7.57 (1H, m, Ar–**H**), 7.65 (2H, d, *J* = 8.7 Hz, Ar–**H**), 7.76 (1H, d, *J* = 7.6 Hz, Ar–**H**), 7.96–8.01(1H, m, Ar–**H**) ppm; ^{13}C NMR (100 MHz, DMSO-d_6): δ 31.8, 41.1, 46.8, 55.8, 56.1, 59.2,66.0, 104.6, 108.3, 115.2, 125.1, 126.1, 128.3, 130.4, 131.5, 132.2, 132.7, 137.9, 144.9, 148.8, 149.4, 150.1, 150.2, 155.1, 192.2 ppm; Anal. Calcd. For $C_{29}H_{32}ClN_3O_3$ (506.05): C 68.83, H 6.37, N 8.30; Found: C 68.75, H 6.29, N 8.41%.

*4.5.8. 2,3-Dihydro-5,6-dimethoxy-2-[4-(4-propyl-4-methylpiperazinium-1-yl)benzylidine]-1H-inden-1-one bromide (**10h**)*

From 0.097 g of 1-Bromopropane as reactant, 0.1 g of yellow solid was obtained (77% yield); mp. 247–251 °C; FT-IR (KBr): ν 2953 (C–H), 2837 (C–H), 1672 (C=O), 1587–1500 (C=C), 1304 (C–N), 1236(C–O) cm^{-1}; ^{1}H NMR (400 MHz, DMSO-d_6): δ 0.93 (3H, t, *J* = 7.3 Hz, C**H**$_3$), 1.70–1.77 (2H, m, C**H**$_2$), 3.15 (3H, s, C**H**$_3$), 3.42–3.46 (2H, m, N–C**H**$_2$), 3.54–3.61 (6H, m, N–C**H**$_2$), 3.71–3.77 (2H, m, N–C**H**$_2$), 3.83 (3H, s, O–C**H**$_3$), 3.90 (3H, s, O–C**H**$_3$), 3.95 (2H, s, C**H**$_2$), 7.12 (2H, d, *J* = 8.8 Hz, Ar–**H**), 7.21 (2H, d, *J* = 6.5 Hz, Ar–**H**), 7.37 (1H, s, =C**H**), 7.67 (2H, d, *J* = 8.9 Hz, Ar–**H**) ppm; ^{13}C NMR (100 MHz, DMSO-d_6): δ 10.4, 14.6, 31.6, 40.8, 45.9, 55.6, 55.9, 58.5, 63.9, 104.4, 108.0, 114.9, 125.9, 130.2, 131.2, 131.9, 132.5, 144.6, 149.2, 149.9, 154.9, 191.7 ppm; Anal. Calcd. For $C_{26}H_{33}BrN_2O_3$ (501.465): C 62.27, H 5.59, N 5.58; Found: C 62.34, H 6.62, N 5.59%.

*4.5.9. 2,3-Dihydro-5,6-dimethoxy-2-[4-(4-butyl-4-methylpiperazinium-1-yl)benzylidine]-1H-inden-1-one bromide (**10i**)*

From 0.108 g of 1-Bromobutane as reactant, 0.12 g of yellow solid was obtained (90% yield); mp. 247–250 °C; FT-IR (KBr): ν 2959 (C–H), 2865 (C–H), 1675 (C=O), 1593–1504 (C=C), 1301 (C–N), 1252 (C–O) cm^{-1}; ^{1}H NMR (400 MHz, DMSO-d_6): δ 0.95 (3H, t, *J* = 7.4 Hz, C**H**$_3$), 1.32–1.38 (2H, m, C**H**$_2$), 1.66–1.74 (2H, m, C**H**$_2$), 3.14 (3H, s, C**H**$_3$), 3.45–3.49 (2H, m, N–C**H**$_2$), 3.54–3.61 (5H, m, N–C**H**$_2$), 3.74 (2H, br, N–C**H**$_2$), 3.83 (3H, s, O–C**H**$_3$), 3.90 (3H, s, O–C**H**$_3$), 3.95 (2H, s, C**H**$_2$), 7.12 (2H, d, *J* = 8.8 Hz, Ar–**H**), 7.21 (2H, d, *J* = 6.8 Hz, Ar–**H**), 7.38 (1H, s, =C**H**), 7.67 (2H, d, *J* = 8.8 Hz, Ar–**H**) ppm; ^{13}C NMR (100 MHz, DMSO-d_6): δ 13.5, 19.2, 23.0, 31.7, 40.9, 45.8, 55.7, 56.0, 58.6, 62.6, 104.5, 108.2, 115.0, 126.0, 130.3, 131.3, 132.07, 132.1, 132.5, 144.7, 150.0, 155.0, 191.9 ppm; Anal. Calcd. For $C_{27}H_{35}BrN_2O_3$ (515.49): C 62.91, H 6.84, N 5.43; Found: C 62.56, H 6.83, N 5.42%.

*4.5.10. 2,3-Dihydro-5,6-dimethoxy-2-[4-(4-pentyl-4-methylpiperazinium-1-yl)benzylidine]-1H-inden-1-one bromide (**10j**)*

From 0.119 g of 1-Bromopentane as reactant, 0.11 g of yellow solid was obtained (80% yield); mp. > 250 °C; FT-IR (KBr): ν 2943 (C–H), 2859 (C–H), 1675 (C=O), 1589–1497 (C=C), 1299 (C–N), 1251(C–O) cm^{-1}; ^{1}H NMR (400 MHz, DMSO-d_6): δ 0.90 (3H, t, *J* = 7.2 Hz, C**H**$_3$), 1.26–1.39 (4H, m, C**H**$_2$), 1.69–1.76 (2H, m, C**H**$_2$), 3.14 (3H, s, C**H**$_3$), 3.44–3.48 (2H, m, N–C**H**$_2$), 3.54–3.60 (6H, m, N–C**H**$_2$), 3.74–3.75 (2H, m, N–C**H**$_2$), 3.82 (3H, s, O–C**H**$_3$), 3.89 (3H, s, O–C**H**$_3$), 3.95 (2H, s, C**H**$_2$), 7.12 (2H, d, *J* = 8.8 Hz, Ar–**H**), 7.21 (2H, d, *J* = 6.0 Hz, Ar–**H**), 7.37 (1H, s, =C**H**), 7.67 (2H, d, *J* = 8.8 Hz, Ar–**H**) ppm; ^{13}C NMR (100 MHz, DMSO-d_6): δ 13.7, 20.6, 21.7, 27.9, 31.7, 40.9, 45.8, 55.7, 56.0, 58.5, 62.8, 104.5, 108.1, 115.0, 126.0, 130.3, 131.3, 132.0, 132.6, 132.9, 144.7, 149.3, 150.0, 155.0, 191.9 ppm; Anal. Calcd. For $C_{28}H_{37}BrN_2O_3$ (529.52): C 63.51, H 7.04, N 5.29; Found: C 63.55, H 7.01, N 5.23%.

*4.5.11. 2,3-Dihydro-5,6-dimethoxy-2-[4-(4-hexyl-4-methylpiperazinium-1-yl)benzylidine]-1H-inden-1-one bromide (**10k**)*

From 0.13 g of 1-Bromohexane as reactant, 0.11 g of yellow solid was obtained (78% yield); mp. > 250 °C; FT-IR (KBr): ν 2927 (C–H), 2858 (C–H), 1674 (C=O), 1591–1497 (C=C), 1300 (C–N), 1248 (C–O) cm^{-1}; ^{1}H NMR (400 MHz, DMSO-d_6): δ 0.86 (3H, t, *J* = 6.6 Hz, C**H**$_3$), 1.30 (6H, m, C**H**$_2$), 1.71 (2H, m, C**H**$_2$), 3.14 (3H, s, C**H**$_3$), 3.50 (2H, m, N–C**H**$_2$), 3.55–3.57 (6H, m, N–C**H**$_2$), 3.74–3.76 (2H, m, N–C**H**$_2$), 3.81 (3H, s, O–C**H**$_3$), 3.88 (3H, s, O–C**H**$_3$), 3.93 (2H, s, C**H**$_2$), 7.11 (2H, d, *J* = 8.8 Hz, Ar–**H**), 7.19 (2H, d, *J* = 12.3 Hz, Ar–**H**), 7.35 (1H, s, =C**H**), 7.65 (2H, d, *J* = 8.8 Hz, Ar–**H**) ppm; ^{13}C NMR (100 MHz, DMSO-d_6): δ 13.8, 20.9, 21.9, 25.4, 30.7, 31.7, 40.9, 45.9, 55.7, 56.0, 58.6, 62.8, 104.5, 108.2, 115.0, 126.0, 130.3, 131.3, 132.0, 132.6, 144.7, 149.2, 150.0, 155.0, 191.9 ppm; Anal. Calcd. For $C_{29}H_{39}BrN_2O_3$ (543.55) C: 64.08, H: 7.23, N: 5.15 Found: C: 63.99, H: 7.20, N: 5.18%.

*4.5.12. 2,3-Dihydro-5,6-dimethoxy-2-[4-(4-(2-propen-1-yl)-4-methylpiperazinium-1-yl)benzylidine]-1H-inden-1-one chloride (**10 l**)*

From 0.06 g of 3-Chloro-1-propene as reactant, 0.09 g of dark yellow solid was obtained (76% yield); mp. 219–223 °C; FT-IR (KBr): ν 2966 (C–H), 2853 (C–H), 1677 (C=O), 1590–1505 (C=C), 1304 (C–N), 1249 (C–O) cm^{-1}; ^{1}H NMR (400 MHz, DMSO-d_6): δ 3.17 (3H, s, C**H**$_3$), 3.58 (5H, br, N–C**H**$_2$), 3.61–3.62 (1H, m, N–C**H**$_2$), 3.76–3.79

(2H, m, N−C**H**$_2$), 3.82 (3H, s, O−C**H**$_3$), 3.89 (3H, s, O−C**H**$_3$), 3.93 (2H, s, C**H**$_2$), 4.25 (2H, d, J = 7.1 Hz, N−C**H**$_2$), 5.65−5.73 (2H, m, =C**H**$_2$), 6.07−6.17 (1H, m, =C**H**), 7.11 (2H, d, J = 8.8 Hz, Ar−**H**), 7.20 (2H, d, J = 7.2 Hz, Ar−**H**), 7.36(1H, s, =C**H**), 7.66 (2H, d, J = 8.8 Hz, Ar−**H**) ppm; ^{13}C NMR (100 MHz, DMSO-d_6): δ 31.6, 40.7, 46.1, 55.6, 55.9, 58.1, 64.4, 104.4, 108.1, 115.0, 125.3, 125.9, 127.9, 130.3, 131.2, 132.0, 132.5132.87, 144.6, 149.2, 149.9, 154.9, 191.8 ppm; Anal. Calcd. For $C_{26}H_{31}ClN_2O_3$ (454.00): C 68.63, H 6.87, N 6.16; Found: C 68.56, H 6.83, N 6.10%.

4.5.13. 2,3-Dihydro-5,6-dimethoxy-2-[4-(4-(2-hydroxyethyl)-4-methylpiperazinium-1-yl)benzylidine]-1H-inden-1-one chloride (**10m**)

From 0.063 g of 2-Chloroethan-1-ol as reactant, 0.1 g of yellow solid was obtained (84% yield); mp. > 250 °C; FT-IR (KBr): ν 2997 (C−H), 2887 (C−H), 1677 (C=O), 1591−1506 (C=C), 1304 (C−N), 1254 (C−O), 1122 (C−O) cm^{-1}; ^{1}H NMR (400 MHz, DMSO-d_6): δ 3.26 (3H, s, C**H**$_3$), 3.65−3.75 (10H, m, N−C**H**$_2$), 3.82 (3H, s, O−C**H**$_3$), 3.89 (3H, s, O−C**H**$_3$), 3.93 (4H, br, C**H**$_2$, O−C**H**$_2$), 5.69 (1H, t, J = 4.8 Hz, O**H**), 7.11 (2H, d, J = 8.5 Hz, Ar−**H**), 7.20 (2H, d, J = 6.5 Hz, Ar−**H**), 7.36 (1H, s, =C**H**), 7.65 (2H, d, J = 8.5 Hz, Ar−**H**) ppm; ^{13}C NMR (100 MHz, DMSO-d_6): δ 29.9, 31.6, 40.8, 47.0, 54.5, 55.6, 55.9, 59.3, 64.0, 104.4, 108.0, 114.5, 114.9, 125.9, 130.3, 131.2, 131.5, 131.9, 132.4, 144.6, 149.2, 149.9, 154.9, 191.7 ppm; Anal. Calcd. For $C_{25}H_{31}ClN_2O_4$ (458.99): C 65.42, H 6.81, N 6.10; Found: C 65.50, H 6.77, N 6.16%.

4.6. General procedure for the synthesis of compounds **10n-o** [1,48]

The mixture of compound **8** (0.098 g, 0.26 mmol) and compound **9a-b** (0.26 mmol) in acetonitrile (5 ml) was refluxed for 24 h. The precipitate was filtered and washed with acetonitrile, and then the solid product was dried under vacuum.

4.6.1. 2,3-Dihydro-5,6-dimethoxy-2-[4-(4-((2,3-dihydro-5,6-dimethoxy-1H-inden-1-one-2-(4-ethoxybenzylidine-2-yl))-4-methylpiperazinium-1-yl)benzylidine]-1H-inden-1-one bromide (**10n**)

From 0.1 g of 2,3-dihydro-5,6-dimethoxy-2-[4-(2-bromoethoxy) benzylidine]-1*H*-inden-1-one (**9a**) as reactant, 0.11 g of dark yellow solid was obtained (55% yield); mp. 230- 235 °C; FT-IR (KBr): ν 2901 (C−H), 1680 (C=O), 1595−1505 (C=C), 1304 (C−N), 1171(C−O) cm^{-1}; ^{1}H NMR (400 MHz, DMSO-d_6): δ 3.65 (3H, br, C**H**$_3$), 3.73(4H, br, N−C**H**$_2$), 3.830−3.835 (8H, m, O−C**H**$_3$, C**H**$_2$), 3.902 (3H, s, O−C**H**$_3$), 3.908 (3H, s, O−C**H**$_3$), 3.96−3.97 (4H, m, CH$_2$, N−C**H**$_2$), 4.0 (2H, m, N−C**H**$_2$), 4.11−4.14 (2H, m, N−C**H**$_2$), 4.63(2H, m, O−C**H**$_2$), 7.13−7.16 (4H, m, Ar−**H**), 7.20 (1H, s, Ar−**H**), 7.21 (3H, s, Ar−**H**), 7.38 (1H, s, =C**H**), 7.42 (1H, s, =C**H**), 7.66−7.71 (4H, m, Ar−**H**) ppm; ^{13}C NMR (100 MHz, DMSO-d_6): δ 29.9, 31.6, 40.8, 46.9, 55.6, 56.0, 58.6, 61.9, 67.0, 67.5, 104.6, 108.2, 115.1, 115.4, 126.1, 127.7, 128.6, 130.1, 130.3, 131.2, 132.0, 132.4, 132.6, 133.4, 144.6, 144.8, 149.2, 149.9, 155.1, 159.5, 192.2 ppm; Anal. Calcd. For $C_{43}H_{45}BrN_2O_7$ (781.74): C 66.07, H 5.80, N 3.58; Found: C 66.13, H 5.74, N 3.62%.

4.6.2. 2,3-Dihydro-5,6-dimethoxy-2-[4-(4-((2,3-dihydro-5,6-dimethoxy-1H-inden-1-one-2-(4-butoxybenzylidine-4-yl))-4-methylpiperazinium-1-yl)benzylidine]-1H-inden-1-one (**10o**)

From 0.11 g of 2,3-dihydro-5,6-dimethoxy-2-[4-(4-bromobutoxy)benzylidine]-1*H*-inden-1-one (**9b**) as reactant, 0.1 g of yellow solid was obtained (48% yield); mp. 222−218 °C; FT-IR (KBr): ν 2929 (C−H), 2830 (C−H), 1678 (C=O), 1592−1501 (C=C), 1303 (C−N), 1248 (C−O), 1125 (C−O) cm^{-1}; ^{1}H NMR (400 MHz, DMSO-d_6): δ 1.81−1.82 (2H, m, C**H**$_2$), 1.93 (2H, br, C**H**$_2$), 3.17 (3H, s, C**H**$_3$), 3.60 (8H, br, N−C**H**$_2$), 3.71 (2H, br, N−C**H**$_2$), 3.81 (3H, s, O−C**H**$_3$), 3.83 (3H, s, O−C**H**$_3$), 3.89−3.93 (10H, m, O−C**H**$_3$, N−C**H**$_2$), 4.13−4.15 (2H, m, O−C**H**$_2$), 7.06−7.12 (4H, m, Ar−**H**), 7.18−7.19 (4H, m, Ar−**H**), 7.37 (1H, s, =C**H**), 7.40 (1H, s, =C**H**$_2$), 7.65−7.71 (4H, m, Ar−**H**) ppm; ^{13}C NMR (100 MHz, DMSO-d_6): δ 18.1, 25.4, 31.5, 31.7, 40.8, 46.2, 55.6, 56.0, 58.6, 61.9, 67.0, 67.4, 104.5, 108.0, 115.0, 115.10, 126.1, 127.8, 128.6, 130.1, 130.3, 131.0, 131.2, 132.0, 132.3, 132.6, 133.4, 144.6, 144.8, 149.3, 149.9, 155.14, 159.5, 191.8 ppm. Anal. Calcd. For $C_{45}H_{49}BrN_2O_7$ (809.80): C 66.74, H 6.10, N 3.46; Found: C 66.79, H 6.05, N 3.41%.

4.7. Biochemical studies. Cholinesterase inhibitory activities

Ellman's method [49] was used to measure the inhibitory activities of newly synthesized compounds and obtained the value of the 50% inhibitory concentration (IC_{50}) for in vitro hAChE and hBuChE inhibitory activity of these compounds. In this method, human erythrocytes AChE and human plasmatic BuChE were produced from fresh blood [60]. 5, 5′-dithiobis (2-nitrobenzoic acid) (Ellman's reagent, DTNB), phosphate buffer (PB, pH 7.4), acetylthiocholine (ATC) and butylthiocholine (BTC) were purchased from Sigma-Aldrich. Glass cuvettes were used for measuring purposes. All tests were carried out in sodium phosphate buffer (0.1 M of Na_2HPO_4 with pH = 8), 5, 5′-dithiobis (2-nitrobenzoic acid) (DTNB, Ellman's reagent) (3.5 mM, in Na_2HPO_4 buffer with pH = 7) and acetylthiocholine iodide (7 mM, in Na_2HPO_4 buffer with pH = 8) as the substrates of the enzymatic reaction. The inhibitory activities of synthesized derivatives were obtained in five different concentrations, and to get repeatability, each experiment was carried out twice. The assay medium (1 ml) consisted of 550 μL of phosphate buffer (pH = 8), 150 μL of DTNB, 150 μL of substrate and 150 μL of inhibitor (10^{-4} - 10^{-10} M) in test cuvettes, and 700 μL of phosphate buffer (pH = 8), 150 μL of DTNB and 150 μL of inhibitor (10^{-4} - 10^{-10} M) in control cuvettes were incubated for 5 min in 37 °C. The reaction was initiated by the immediate addition of 50 μL of the enzyme. The activity was determined by measuring the increase in absorbance at 412 nm in 5 min intervals using a spectrophotometer Helios-Zeta (Thermospectronic, Cambridge, U.K.). hBuChE study was conducted in a similar situation described above. Non-linear and linear regressions were used to estimate the drug concentrations inducing 50% inhibition of the hAChE or hBuChE activity [45].

4.8. Kinetic evaluation of compounds **10a** and **10e** on hAChE and hBuChE inhibitions

The kinetic studies were performed at five different concentrations of the acetylthiocholine iodide (0.1−1 mM) and butyrilthiocholine iodide (0.1−1 mM) substrates for hAChE and hBuChE enzymes, respectively. The spectrometric Ellman's method was used for measuring the velocity of enzymatic reaction for compounds **10a** and **10e** [49]. In each case, two different concentrations of tested compound **10a** were used to investigate the mechanism of hAChE (5×10^{-7} and 5×10^{-6} mM) and hBuChE (5×10^{-7} and 10^{-6} mM) inhibitions. Another two different concentrations of compound **10e** were used for the kinetic evaluation of hAChE (5×10^{-7} and 10^{-6} mM) and hBuChE (510^{-7} and 710^{-7} mM) inhibitions. To obtain inhibition constants; i.e. Ki and KI values for AChE and BuChE, reciprocal plots of 1/V vs. 1/[S] and 1/Vapp vs. inhibitor concentration were drawn respectively (Lineweaver−Burk plot) [61]. Data analysis was performed with Microsoft Excel software.

4.9. Evaluation of cytotoxicity in vitro

The cytotoxicity of the test compounds was determined in human foreskin fibroblast (HFF) cells, MCF-7 cells and neuronal SH-SY5Y cells using the 3-(4,5-dimethylthiazol-2-yl)-2,5-diphenyl tetrazolium bromide (MTT) assay. MTT is reduced to formazan by the

mitochondrial activity of viable cells. HFF, MCF-7 and SH-SY5Y cells from the Pasteur Institute of Iran were purchased and cultured. The cells were seeded at a concentration of 10^4 cells/well, into a 96-well plate, in each well. After 24 h of incubation, in each well distributed 200 μL of test compounds at different final concentrations (7.8–1000 μM) and incubated at 37 °C in 5% CO_2 for 48 h. At the end of the treatment, 10 μL of MTT (2 mg/ml) was added and the cells were incubated again for an additional 4 h period. Then, the medium was carefully removed and 200 μL of DMSO was added for solubilization of formazan crystals in each well. The amount of formazan was measured at 570 nm using an awareness technology (Florida, USA) at 570 nm with a reference wavelength of 630 nm. In all determinations, cytotoxicity is expressed as the concentration of the compound resulting in 50% inhibition of cell viability.

4.10. Aβ toxicity

The experiment was done on 7-day-old cultures of PC12. PC12 cells were grown up in Dulbecco's modified Eagle's medium (DMEM) with 7% fetal bovine serum, 7% horse serum, 100 mg/ml streptomycin, and 100 units/ml penicillin [62]. Then the cells were incubated with 5 μM Aβ (1–42) ((rat/mouse) ab120959), in DMEM without serum. The plates were transferred to a 5% CO_2 incubator and incubated at 37°C for 24 h. Then compound **10e** with concentration of 1 μM and 10 μM was added to the incubation and incubated for 24 h [63].

4.11. Measurement of the ROS production

4.11.1. DCFH-DA assay

The level of ROS was quantified using the 2′,7′-dichlorofluorescein-diacetate (DCFH-DA). In DCFH-DA assay, the cells of each group were incubated with 10 μM of DCFH-DA for 15 min at room temperature to allow the DCFH-DA to be incorporated into any membrane-bound vesicles and also to let the diacetate group be cleaved by esterases. Then the nuclei of cells were counterstained with DAPI and observed under a fluorescent microscope with excitation at 358 nm/emission at 461 nm and the converted DCF product was measured using the multiple readers with a fluorescence spectrophotometer, excitation at 485 nm and emission at 530 nm. The fluorescence was measured using a fluorescence spectrometer Thermoscintific- Finland Multiscan spectrophotometer (GO MULTISCAN).

4.11.2. Tunnel assay

Several apoptotic cells were detected by Tunnel assay. In TUNEL assay cells were fixed in 4% paraformaldehyde in PBS and pH 7.4 for 1 h at room temperature, slides were washed in PBS and incubated with blocking solution (methanol 3% in H_2O_2) for 10 min at room temperature. Then again washed with PBS and incubated with 0.1% Triton X-100 in 0.1% sodium Citra for 2 min in ice. Slides were washed twice with PBS. In a wet pan, 50 μL of the reaction mixture was added to each sample and then incubate at 37 °C for 60 min. Slides were washed three times with PBS. Then the nuclei of cells were stained with DAPI and observed under a fluorescent microscope with excitation at 500–550 nm/emission at 565-515 nm and excitation at 358 nm/emission at 461 nm for fluorcein fluorescent and DAPI, respectively. Using a fluorescence spectrometer Thermoscintific- Finland Multiscan spectrophotometer (GO MULTISCAN).

4.12. Malonyl dialdehyde (MDA) analysis

MDA is produced by a breakdown of the oxidative of cell membrane lipids and it is an index of lipid peroxidation. We measured lipid peroxidation induced by Aβ (5 μM) with or without **10e** (1 μM and 10 μM) after 8 h of incubation. Using a thiobarbituric acid reactive substance (TBARS) assay kit was measured intracellular MDA production. 1- 10^6 cells per well were seeded in a six-well plate, then collected in 200 ml of culture medium and sonicated for 3×5 s intervals at 40 V over ice. SDS Lysis solution (100 ml) was added to the sample solution and mixed thoroughly. Then, 250 ml of TBA reagent were added and incubated at 95 °C for 45–60 min. After loading into a clear 96-well plate and the absorbance at 535 nm was recorded using a microplate reader (Thermoscintific- Finland Multiscan spectrophotometer (GO MULTISCAN) [53,64].

4.13. Determination of lactate dehydrogenase (LDH)

LDH release is an indicator of neuronal injury and obtained according to the percentage leakage of LDH into the culture medium to the total LDH activity per culture. Lactate dehydrogenase (LDH) levels were measured in the culture medium after induction of cytoxicity with Aβ with and without **10e**. Lactate dehydrogenase (LDH) activity is according to the below reaction:

$$\text{Piruvate} + \text{NADH} \xrightarrow{LDH} \text{Lactate} + \text{NAD}^+$$

that results from the oxidation of NADH and it is measured as the rate of decrease in the absorbance at 340 nm, using a Thermoscintific- Finland Multiscan spectrophotometer (GO MULTISCAN) [53,65].

4.14. TAC assay

From the solution consists of 10 mM phosphate-buffered saline (pH 7.2), 50 μl of myoglobin solution, 20 μl of 3 mM ABTS solution (final concentration: 300 μM), and 20 μl of diluted plasma or Trolox solution, 90 μL removed and added to 8 wells of 96-well microplate, mixed by vibration, and maintained at 25 °C for 3 min. After the addition of Aβ, the reaction started at 450 nm with the microplate reader (Thermoscintific- Finland Multiscan spectrophotometer (GO MULTISCAN)) for 5 min (25 °C) [66].

4.15. Anti-inflammatory assay

4.15.1. Gene expression analysis

mRNA expressions of the IL-1β and TNF-α genes were measured by real-time PCR using the SYBR Green method. RNX-PLUS solution was used to isolate total RNA (SinaClon, Tehran, Iran), and complementary DNA (cDNA) was synthesized using a Revert Aid Reverse Transcriptase Kit (Thermo Fisher, Waltham, MA, USA). Beta actin was considered as an endogenous control for mRNA. The $2-\Delta\Delta CT$ method was applied to calculate gene expressions relative to the housekeeping control of Beta actin.

4.15.2. Statistical analysis

Statistical analysis was done by SPSS software (version 23.0; SPSS Inc). Data analysis of four studied groups was carried out by repeated measure One-Way ANOVA test. For graphs illustration, version 7.00 of GraphPad Prism software (GraphPad Software, La Jolla, CA, USA, www.graph pad.com) was used. $p < 0.05$ was considered to be statistically significant.

4.16. Molecular docking studies

Human AchE (pdb 4Ey7), human BuchE (pdb 1p0p) and Aβ (1-42) (pdb 1iYT) were obtained from the Protein Data Bank [22,67–71]. MGL tools 1.5.6 with AutoGrid4 and AutoDock4 were

used to set up and perform docking simulation [72,73]. Using AutoDock Tools, target and ligand files were provided. Water molecules were removed first of all. To perform docking calculations, Lamarckian genetic algorithms were employed as they are implemented in AutoDock. The lowest energy docked conformation obtained from the AutoDock function was selected as the binding mode. The relevant output resulting from AutoDock was illustrated by Discovery studio 4.5.

Declaration of competing interest

The authors declare that they have no known competing financial interests or personal relationships that could have appeared to influence the work reported in this paper.

Acknowledgements

This project was financially supported by a grant from Iran National Science Foundation (INSF) (ID No. 97015588). The authors would like to acknowledge the financial support from University of Tabriz, Tabriz University of medical sciences and the Deputy for Research and Technology of Iranian Ministry of Health and Medical Education.

Appendix A. Supplementary data

Supplementary data to this article can be found online at https://doi.org/10.1016/j.ejmech.2020.112140.

References

[1] L. Peauger, R. Azzouz, V. Gembus, M.L. Tintas, J. Sopková-de Oliveira Santos, P. Bohn, C. Papamicaël, V. Levacher, Donepezil-based central acetylcholinesterase inhibitors by means of a "bio-oxidizable" prodrug strategy: design, synthesis, and in vitro biological evaluation, J. Med. Chem. 60 (2017) 5909–5926, https://doi.org/10.1021/acs.jmedchem.7b00702.

[2] A. Association, Alzheimer's disease facts and figures, Alzheimers Dement 10 (2014) (2014) e47–e92, https://doi.org/10.1016/j.jalz.2014.02.001.

[3] B. Yiğit, M. Yiğit, D. Barut Celepci, Y. Gök, A. Aktas, M. Aygun, P. Taslimi, I. Gulcin, Novel benzylic substituted imidazolinium, tetrahydropyrimidinium and tetrahydrodiazepinium salts: potent carbonic anhydrase and acetylcholinesterase inhibitors, Chemistry 3 (2018) 7976–7982, https://doi.org/10.1002/slct.201801019.

[4] A. Mohammadi-Farani, A. Ahmadi, H. Nadri, A. Aliabadi, Synthesis, docking and acetylcholinesterase inhibitory assessment of 2-(2-(4-Benzylpiperazin- 1-yl)ethyl)isoindoline-1,3-dione derivatives with potential anti-Alzheimer effects, *DARU* J. Pharm. Sci. 21 (2013) 47, https://doi.org/10.1186/2008-2231-21-47.

[5] X. Zhang, X. He, Q. Chen, J. Lu, S. Rapposelli, R. Pi, A review on the hybrids of hydroxycinnamic acid as multi-targetdirected ligands against Alzheimer's disease, Bioorg. Med. Chem. 26 (2018) 543–550, https://doi.org/10.1016/j.bmc.2017.12.042.

[6] K.S.T. Dias, C.T. de Paula, T. dos Santos, I.N. Souza, M.S. Boni, M.J. Guimarães, F.M. da Silva, N.G. Castro, G.A. Neves, C.C. Veloso, M.M. Coelho, I. Souza D. Melo, F.C.V. Giusti, A. Giusti-Paiva, M.L. da Silva, L.E. Dardenne, I.A. Guedes, L. Pruccoli, F. Morroni, A. Tarozzi, C. Viegas Jr., Design, synthesis and evaluation of novel feruloyl-donepezil hybrids as potential multitarget drugs for the treatment of Alzheimer's disease, Eur. J. Med. Chem. 130 (2017) 440–457, https://doi.org/10.1016/j.ejmech.2017.02.043.

[7] H. Watanabe, M. Ono, H. Kimura, S. Kagawa, R. Nishii, T. Fuchigami, M. Haratake, M. Nakayama, H. Saji, A dual fluorinated and iodinated radiotracer for PET and SPECT imaging of b-amyloid plaques in the brain, Bioorg. Med. Chem. Lett 21 (2011) 6519–6522, https://doi.org/10.1016/j.bmcl.2011.08.063.

[8] G.-F. Zha, C.-P. Zhang, H.-L. Qin, I. Jantan, M. Sher, M.W. Amjad, M.A. Hussain, Z. Hussain, S.N.A. Bukhari, Biological evaluation of synthetic a,b-unsaturated carbonyl based cyclohexanone derivatives as neuroprotective novel inhibitors of acetylcholinesterase, butyrylcholinesterase and amyloid-b aggregation, Bioorg. Med. Chem. 24 (2016) 2352–2359, https://doi.org/10.1016/j.bmc.2016.04.015.

[9] S. Nasir Abbas Bukhari, I. Jantan, Synthetic curcumin analogs as inhibitors of β -Amyloid peptide aggregation: potential therapeutic and diagnostic agents for Alzheimer's disease, Mini Rev. Med. Chem. 15 (2015) 1110–1121.

[10] D.J. Selkoe, Alzheimer's disease: genes, proteins, and therapy, Physiol. Rev. 81 (2001) 741–766, https://doi.org/10.1152/physrev.2001.81.2.741.

[11] J.H. Lange, H.K. Coolen, M.A. van der Neut, A.J. Borst, B. Stork, P.C. Verveer, C.G. Kruse, Design, synthesis, biological properties, and molecular modeling investigations of novel tacrine derivatives with a combination of acetylcholinesterase inhibition and cannabinoid CB1 receptor antagonism, J. Med. Chem. 53 (2010) 1338–1346, https://doi.org/10.1021/jm901614b.

[12] X. Zha, D. Lamba, L. Zhang, Y. Lou, C. Xu, D. Kang, L. Chen, Y. Xu, L. Zhang, A. De Simone, S. Samez, A. Pesaresi, J. Stojan, M.G. López, J. Egea, V. Andrisano, M. Bartolini, Novel tacrine-benzofuran hybrids as potent multitarget-directed ligands for the treatment of Alzheimer's Disease: design, synthesis, biological evaluation and x-ray crystallography, J. Med. Chem. (2015) 2–67, https://doi.org/10.1021/acs.jmedchem.5b01119.

[13] Q. Li, S. He, Y. Chen, F. Feng, W. Qu, H. Sun, Donepezil-based multi-functional cholinesterase inhibitors for treatment of Alzheimer's disease, Eur. J. Med. Chem. 158 (2018) 463–477, https://doi.org/10.1016/j.ejmech.2018.09.031.

[14] Z. Haghighijoo, O. Firuzi, B. Hemmateenejad, S. Emami, N. Edraki, R. Miri, Synthesis and biological evaluation of quinazolinone-based hydrazones with potential use in Alzheimer's disease, Bioorg. Chem. 74 (2017) 126–133, https://doi.org/10.1016/j.bioorg.2017.07.014.

[15] L. Jalili-Baleh, E. Babaei, S. Abdpour, S.N.A. Bukhari, A. Foroumadi, A. Ramazani, M. Sharifzadeh, M. Abdollahi, M. Khoobi, A review on flavonoid-based scaffolds as multi-target-directed ligands (MTDLs) for Alzheimer's disease, Eur. J. Med. Chem. 152 (2018) 570–589, https://doi.org/10.1016/j.ejmech.2018.05.004.

[16] K.O. Yerdelen, M. Koca, B. Anil, H. Sevindik, Z. Kasap, Z. Halici, K. Turkaydin, G. Gunesacar, Synthesis of donepezil-based multifunctional agents for the treatment of Alzheimer's disease, Bioorg. Med. Chem. Lett 25 (2015) 5576–5582, https://doi.org/10.1016/j.bmcl.2015.10.051.

[17] Y. Özkay, Ü.D. Özkay, Acetylcholine esterase inhibitory potential of some benzimidazole derivatives, EIJST 3 (2014) 115–120.

[18] J. Leng, H.L. Qin, K. Zhu, I. Jantan, M.A. Hussain, M. Sher, M.W. Amjad, M. Naeem -ul -Hassan, W. Ahmad, S.N.A. Bukhari, Evaluation of multifunctional synthetic tetralone derivatives for treatment of Alzheimer's disease, Chem. Biol. Drug Des. 88 (2016) 889–898, https://doi.org/10.1111/cbdd.12822.

[19] S.N.A. Bukhari, I. Jantan, V.H. Masand, D.T. Mahajan, M. Sher, M. Naeem-ul-Hassan, M.W. Amjad, Synthesis of a, b-unsaturated carbonyl based compounds as acetylcholinesterase and butyrylcholinesterase inhibitors: characterization, molecular modeling, QSAR studies and effect against amyloid b-induced cytotoxicity, Eur. J. Med. Chem. 83 (2014) 355–365, https://doi.org/10.1016/j.ejmech.2014.06.034.

[20] Y. Wu, Q. Xu, W. Song, Oxidative stress and Alzheimer's disease, Syst. Biol. Free Radicals Antioxid. 95 (2014) 2147–2174, https://doi.org/10.1007/978-3-642-30018-9-197.

[21] M. Shidore, J. Machhi, K. Shingala, P. Murumkar, M.K. Sharma, N. Agrawal, A. Tripathi, Z. Parikh, P. Pillai, M.R. Yadav, Benzylpiperidine-linked diarylthiazoles as potential anti-Alzheimer's agentssynthesis and biological evaluation, J. Med. Chem. 59 (2016) 5823–5846, https://doi.org/10.1021/acs.jmedchem.6b00426.

[22] J. Cheung, M.J. Rudolph, F. Burshteyn, M.S. Cassidy, E.N. Gary, J. Love, M.C. Franklin, J.J. Height, Structures of human acetylcholinesterase in complex with pharmacologically important ligands, J. Med. Chem. 55 (2012) 10282–10286, https://doi.org/10.1021/jm300871x.

[23] E. Sawatzky, S. Wehle, B. Kling, J. Wendrich, G. Bringmann, C.A. Sotriffer, J. Heilmann, M. Decker, Discovery of highly selective and nanomolar carbamate-based butyrylcholinesterase inhibitors by rational investigation into their inhibition mode, J. Med. Chem. 59 (2016) 2067–2082, https://doi.org/10.1021/acs.jmedchem.5b01674.

[24] H. Akrami, B.F. Mirjalili, M. Khoobi, H. Nadri, A. Moradi, A. Sakhteman, S. Emami, A. Foroumadi, A. Shafiee, Indolinone-based acetylcholinesterase inhibitors: synthesis, biological activity and molecular modeling, Eur. J. Med. Chem. 12 (2014) 375–381, https://doi.org/10.1016/j.ejmech.2014.01.017.

[25] I. Buendia, J. Egea, E. Parada, E. Navarro, R. León, M.I. Rodríguez-Franco, M.G. López, The melatonin–N,N-dibenzyl(N-methyl)amine hybrid ITH91/IQM157 affords neuroprotection in an in vitro Alzheimer's model via hemooxygenase-1 induction, ACS Chem. Neurosci. 6 (2015) 288–296, https://doi.org/10.1021/cn50020731.

[26] R. Azzouz, L. Peauger, V. Gembus, M.L. Tîntas, J. Sopková-de Oliveira Santos, C. Papamicael, V. Levacher, Novel donepezil-like N-benzylpyridinium salt derivatives as AChE inhibitors and their corresponding dihydropyridine "bio-oxidizable" prodrugs: synthesis, biological evaluation and structure-activity relationship, Eur. J. Med. Chem. 145 (2018) 165–190, https://doi.org/10.1016/j.ejmech.2017.12.084.

[27] L. Monjas, M.P. Arce, R. León, J. Egea, C. Pérez, M. Villarroya, M.G. López, C. Gil, S. Conde, M.I. Rodríguez-Franco, Enzymatic and solid-phase synthesis of new donepezil-based L- and D-glutamic acid derivatives and their pharmacological evaluation in models related to Alzheimer's disease and cerebral ischemia, Eur. J. Med. Chem. **130** (2017) 60–72, https://doi.org/10.1016/j.ejmech.2017.02.034.

[28] A.M. Kanhed, A. Sinha, J. Machhi, A. Tripathi, Z.S. Parikh, P.P. Pillai, R. Giridhar, M.R. Yadav, Discovery of isoalloxazine derivatives as a new class of potential anti-Alzheimer agents and their synthesis, Bioorg. Chem. 61 (2015) 7–12, https://doi.org/10.1016/j.bioorg.2015.05.005.

[29] S. Hamulakova, L. Janovec, M. Hrabinova, K. Spilovska, J. Korabecny, P. Kristian, K. Kuca, J. Imrich, Synthesis and biological evaluation of novel tacrine derivatives and tacrine–coumarin hybrids as cholinesterase inhibitors,

J. Med. Chem. 57 (2014) 7073–7084, https://doi.org/10.1021/jm5008648.
[30] I. Łozińska, A. Świerczyńska, Z. Molęda, A.M. Hartman, A.K. Hirsch, Z. Czarnocki, Donepezil–melatonin hybrids as butyrylcholinesterase inhibitors: improving binding affinity through varying mode of linking fragments, Arch. Pharm. Chem. Life Sci. 351 (2018) 1–10, https://doi.org/10.1002/ardp.201800194.
[31] Y. Li, X. Qiang, Y. Li, X. Yang, L. Luo, G. Xiao, Z. Cao, Z. Tan, Y. Deng, Pterostilbene-O-acetamidoalkylbenzylamines derivatives as novel dual inhibitors of cholinesterase with anti-b-amyloid aggregation and antioxidant properties for the treatment of Alzheimer's disease, Bioorg. Med. Chem. Lett 26 (2016) 2035–2039, https://doi.org/10.1016/j.bmcl.2016.02.079.
[32] J.S. Lan, T. Zhang, Y. Liu, J. Yang, S.S. Xie, J. Liu, Z.Y. Miao, Y. Ding, Design, synthesis and biological activity of novel donepezil derivatives bearing N-benzyl pyridinium moiety as potent and dual binding site acetylcholinesterase inhibitors, Eur. J. Med. Chem. 133 (2017) 184–196, https://doi.org/10.1016/j.ejmech.2017.02.045.
[33] L.W. Mohamed, S.M. Abuel-Maaty, W.A. Mohammed, M.A. Galal, Synthesis and biological evaluation of new oxopyrrolidine derivatives as inhibitors of acetyl cholinesterase and β amyloid protein as anti-Alzheimer's agents, Bioorg. Chem. 76 (2018) 210–217, https://doi.org/10.1016/j.bioorg.2017.11.008.
[34] I. Baysal, G. Ucar, M. Gultekinoglu, K. Ulubayram, S. Yabanoglu-Ciftci, Donepezil loaded PLGA-b-PEG nanoparticles: their ability to induce destabilization of amyloid fibrils and to cross blood brain barrier in vitro, J. Neural. Transm. 124 (2017) 33–45, https://doi.org/10.1007/s00702-016-1527-4.
[35] P. Piplani, A. Jain, D. Devi, Anjali, A. Sharma, P. Silakari, Design, synthesis and pharmacological evaluation of some novel indanone derivatives as acetylcholinesterase inhibitors for the management of cognitive dysfunction, Bioorg. Med. Chem. 26 (2018) 215–224, https://doi.org/10.1016/j.bmc.2017.11.033.
[36] H.O. Saxena, U. Faridi, S. Srivastava, J.K. Kumar, M.P. Darokar, S. Luqman, C.S. Chanotiya, V. Krishna, A.S. Negi, S.P.S. Khanuja, Gallic acid-based indanone derivatives as anticancer agents, Bioorg. Med. Chem. Lett 18 (2008) 3914–3918. https://doi:10.1016/j.bmcl.2008.06.039.
[37] X.B. Chen, X.M. Liu, R. Huang, S.J. Yan, J. Lin, Three-component synthesis of indanone-fused spirooxindole derivatives, Eur. J. Org Chem. 2013 (2013) 4607–4613. https://DOI:10.1002/ejoc.201300376.
[38] R. Teimuri-Mofrad, R. Nikbakht, M. Gholamhosseini-Nazari, A convenient and efficient method for the synthesis of new 2-(4-amino substituted benzilidine) indanone derivatives, Res. Chem. Intermed. (2016). https://doi:10.1007/s11164-016-2549-0.
[39] C.B. Mishra, S. Kumari, A. Manral, A. Prakash, V. Saini, A.M. Lynn, M. Tiwari, Design, synthesis, in-silico and biological evaluation of novel donepezil derivatives as multi target-directed ligands for the treatment of Alzheimer's disease, Eur. J. Med. Chem. 125 (2017) 736–750, https://doi.org/10.1016/j.ejmech.2016.09.057.
[40] S. Kumari, C.B. Mishra, M. Tiwari, Design, synthesis and pharmacological evaluation of N-[4-(4-(alkyl/aryl/heteroaryl)-piperazin-1-yl)-phenyl]-carbamic acid ethyl ester derivatives as novel anticonvulsant agents, Bioorg. Med. Chem. Lett 25 (2015) 1092–1099, https://doi.org/10.1016/j.bmcl.2015.01.004.
[41] P. Chaudhary, R. Kumar, A.K. Verma, D. Singh, V. Yadav, A.K. Chhillar, G.L. Sharma, R. Chandra, Synthesis and antimicrobial activity of N-alkyl and N-aryl piperazine derivatives, Bioorg. Med. Chem. 14 (2006) 1819–1826. https://doi:10.1016/j.bmc.2005.10.032.
[42] S. Kumari, C.B. Mishra, M. Tiwari, Pharmacological evaluation of novel 1-[4-(4 benzo[1,3] dioxol-5-ylmethyl-piperazin-1-yl)-phenyl]-3-phenyl-ure as potent anticonvulsant and antidepressant agent, Pharmacol. Rep. 68 (2016) 250–258, https://doi.org/10.1016/j.pharep.2015.08.013.
[43] C.B. Mishra, S. Kumari, M. Tiwari, Design and synthesis of some new 1-phenyl-3/4-[4-(aryl/heteroaryl/alkyl-piperazine1-yl)-phenyl-ureas as potent anticonvulsant and antidepressant agents, Arch Pharm. Res. (Seoul) 39 (2016) 603–617, https://doi.org/10.1080/00397911.2018.1492726.
[44] K. Rahimpour, R. Nikbakht, A. Aghaiepour, R. Teimuri-Mofrad, Synthesis of 2-(4-amino substituted benzylidene)indanone analogues from aromatic nucleophilic substitution (SNAr) reaction, Synth. Commun. 48 (2018) 2253–2259, https://doi.org/10.1080/00397911.2018.1492726.
[45] S. Mozaffarnia, F. Parsaee, E. Payami, H. Karami, S. Soltani, M.R. Rashidi, R. Teimuri-Mofrad, Design, synthesis and biological assessment of novel 2-(4-alkoxybenzylidine)-2,3-dihydro-5,6-dimethoxy-1*H*-inden-1- one derivatives as hAChE and hBuChE Enzyme inhibitors, Chemistry 4 (2019) 9376–9380, https://doi.org/10.1002/slct.201901973.
[46] D.D. Nan, C.S. Gan, C.W. Wang, J.P. Qiao, X.M. Wang, J.N. Zhou, 6-Methoxy-indanone derivatives as potential probes for b-amyloid plaques in Alzheimer's disease, Eur. J. Med. Chem. 124 (2016) 117–128, https://doi.org/10.1016/j.ejmech.2016.07.069.
[47] J.P. Qiao, C.S. Gan, C.W. Wang, J.F. Ge, D.D. Nan, J. Pan, J.N. Zhou, Novel indanone derivatives as potential imaging probes for b-Amyloid plaques in the brain, Chembiochem 13 (2012) 1652–1662, https://doi.org/10.1002/cbic.201200223.
[48] H. Farrokhi1, S. Mozaffarnia, K. Rahimpour, M.R. Rashidi, R. Teimuri-Mofrad, Synthesis, characterization and investigation of AChE and BuChE inhibitory activity of 1-alkyl-4-[(5,6-dimethoxy-1-indanone-2-yl)methylene]pyridinium halide derivatives, J. Iran. Chem. Soc. (2019), https://doi.org/10.1007/s13738-019-01804-1.
[49] G.L. Ellman, K.D. Courtney, V.J. Andres, R.M. Fesrtherstone, A new and rapid colorimetric determination of acetylcholinesterase activity, *B*iochem. Pharmacol. 7 (1961) 88–95, https://doi.org/10.1016/0006-2952(61)90145-9.
[50] H. Wei, P.R. Leeds, Y. Qian, W. Wei, R.w. Chen, D.M. Chuang, β-Amyloid peptide-induced death of PC 12 cells and cerebellar granule cell neurons is inhibited by long-term lithium treatment, Eur. J. Pharmacol. 392 (2000) 117–123.
[51] T.S. Kim, C.U. Pae1, S.J. Yoon, W.Y. Jang, N.J. Lee, J.J. Kim, S.J. Lee, C. Lee, I.H. Paik, C.U. Lee, Decreased plasma antioxidants in patients with Alzheimer's disease, Int. J. Geriatr. Psychiatr. 21 (2006) 344–348, https://doi.org/10.1002/gps.1469.
[52] S.M. Yatina, S. Varadarajan, D.A. Butterfield, Vitamin E prevents Alzheimer's amyloid β-peptide (1-42)-induced neuronal protein oxidation and reactive oxygen species production, J. Alzheim. Dis. 2 (2000) 123–131.
[53] M.J. Oset-Gasque, M.P. González, J. Pérez-Peña, N. García-Font, A. Romero, J. del Pino, E. Ramos, D. Hadjipavlou-Litina, E. Soriano, M. Chioua, A. Samadi, D.S. Raghuvanshi, K.N. Singh, J. Marco-Contelles, Toxicological and pharmacological evaluation, antioxidant, ADMET and molecular modeling of selected racemic chromenotacrines {11-amino-12-aryl-8,9,10,12-tetrahydro-7H-chromeno[2,3-b]quinolin-3- ols} for the potential prevention and treatment of Alzheimer's disease, Eur. J. Med. Chem. 74 (2014) 491–501, https://doi.org/10.1016/j.ejmech.2013.12.021.
[54] M. Bigl, M.K. Brückner, Th Arendt, V. Bigl, K. Eschrich, Activities of key glycolytic enzymes in the brains of patients with Alzheimer's disease, J. Neural. Transm. 106 (1999) 499–511.
[55] C. Cecchi, C. Fiorillo, S. Sorbi, S. Latorraca, B. Nacmias, S. Bagnoli, P. Nassi, G. Liguri, Oxidative stress and reduced antioxidant defenses in peripheral cells from familial Alzheimer's patients, Free Radic. Biol. Med. 33 (2002) 1372–1379.
[56] M.I. Rodríguez-Franco, M.I. Fernández-Bachiller, C. Pérez, B. Hernández -Ledesma, B. Bartolome, Novel tacrine-melatonin hybrids as dual-acting drugs for Alzheimer Disease, with improved acetylcholinesterase inhibitory and antioxidant properties, J. Med. Chem. 49 (2006) 459–462. https://doi:10.1021/jm050746d.
[57] Y. Feng, X. Wang, Antioxidant therapies for Alzheimer's disease, Oxidative med. cell longevity 2012 (2012) 1–17. https://doi:10.1155/2012/47293.
[58] F.L. Heppner, R.M. Ransohoff, B. Becher, Immune attack: the role of inflammation in Alzheimer disease, Nat. Rev. Neurosci. 16 (2015) 358–372. https://doi:10.1038/nrn3880.
[59] A.C. Allison, R. Cacabelos, V.R. Lombardi, X.A. Álvarez, C. Vigo, Celastrol, a potent antioxidant and anti-inflammatory drug, as a possible treatment for Alzheimer's disease, Prog. Neuro-Psychopharmacol. Biol. Psychiatry 25 (2001) 1341–1357.
[60] G. Karimi, M. Iranshahi, F. Hosseinalizadeh, B. Riahi, A. Sahebkar, Screening of acetylcholinesterase inhibitory activity of terpenoid and coumarin derivatives from the genus ferula, Pharmacologyonline 1 (2010) 566–574.
[61] A. Rampa, A. Bisi, F. Belluti, S. Gobbi, P. Valenti, V. Andrisano, V. Cavrini, A. Cavalli, M. Recanatini, Acetylcholinesterase inhibitors for potential use in Alzheimer's disease: molecular modeling, synthesis and kinetic evaluation of 11*H*-indeno-[1,2-b]-quinolin-10-ylamine derivatives, Bioorg. Med. Chem. 8 (2000) 497–506, https://doi.org/10.1016/S0968-0896(99)00306-5.
[62] P. Lazarovici, M. Oshima, D. Shavit, M. Shibutani, H. Jiang, M. Monshipouri, D. Fink, V. Movsesyan, G. Guroff, Down-regulation of epidermal growth factor receptors by nerve growth factor in PC12 cells is p140trk-, Ras-, and Src-dependent, J. Biol. Chem. 272 (1997) 11026–11034.
[63] S. Akasofu, M. Kimura, T. Kosasa, K. Sawada, H. Ogura, Study of neuroprotection of donepezil, a therapy for Alzheimer's disease, Chem. Biol. Interact. 175 (2008) 222–226, https://doi.org/10.1016/j.cbi.2008.04.045.
[64] A. Russoa, M. Palumboa, C. Alianoa, L. Lempereurb, G. Scotoc, M. Renis, Red wine micronutrients as protective agents in Alzheimer-like induced insult, Life Sci. 72 (2003) 2369–2379. https://doi:10.1016/S0024-3205(03)00123-1.
[65] T. Reed, M. Perluigi, R. Sultana, W.M. Pierce, J.B. Klein, D.M. Turner, R. Coccia, W.R. Markesbery, D.A. Butterfield, Redox proteomic identification of 4-Hydroxy-2-nonenal-modified brain proteins in amnestic mild cognitive impairment: insight into the role of lipid peroxidation in the progression and pathogenesis of Alzheimer's disease, Neurobiol. Dis. 30 (2008) 107–120. https://doi:10.1016/j.nbd.2007.12.007.
[66] Y. Kambayashi1, N.T. Binh1, H.W. Asakura, Y. Hibino, Y. Hitomi, H. Nakamura, K. Ogino, Efficient assay for total antioxidant capacity in human PlasmaUsing a 96-well microplate, J. Clin. Biochem. Nutr. 44 (2009) 46–51, https://doi.org/10.3164/jcbn.08-162.
[67] https://www.rcsb.org/structure/4EY7.
[68] Y. Nicolet, O. Lockridge, P. Masson, J.C. Fontecilla-Camps, F. Nachon, Crystal structure of human Butyrylcholinesterase and of its complexes with substrate and products, J. Biol. Chem. 278 (2003) 41141–41147, https://doi.org/10.1074/jbc.M210241200.
[69] https://www.rcsb.org/structure/1P0P.
[70] O. Crescenzi, S. Tomaselli, R. Guerrini, S. Salvadori, A.M. D'Ursi, P.A. Temussi, D. Picone, Solution structure of the Alzheimer amyloid b-peptide (1–42) in an apolar microenvironment, Eur. J. Biochem. 269 (2002) 5642–5648. https://doi:10.1046/j.1432-1033.2002.03271.x.
[71] https://www.rcsb.org/structure/1iyt.
[72] G.M. Morris, R. Huey, W. Lindstrom, M.F. Sanner, R.K. Belew, D.S. Goodsell, A.J. Olson, AutoDock4 and AutoDockTools4: automated docking with selective receptor flexibility, J. Comput. Chem. 30 (2009) 2785–2791, https://doi.org/10.1002/jcc.21256.
[73] G.M. Morris, R. Huey, A.J. Olson, Using AutoDock for ligand-receptor docking, Curr. Protoc. Bioinform. 1 (2008) 8–14, https://doi.org/10.1002/0471250953.bi0814s1024.